U.S. DEPARTMENT OF COMMERCE
National Technical Information Service

PB-256 046

DYNALIST II, A COMPUTER PROGRAM FOR STABILITY AND DYNAMIC RESPONSE ANALYSIS OF RAIL VEHICLE SYSTEMS

VOLUME I. TECHNICAL REPORT

TRANSPORTATION SYSTEMS CENTER

PREPARED FOR
FEDERAL RAILROAD ADMINISTRATION

FEBRUARY 1975

Technical Report Documentation Page

1. Report No.	2. Government Accession No.	3. Recipient's Catalog No.
FRA-OR&D-75-22.I		

4. Title and Subtitle
DYNALIST II, A COMPUTER PROGRAM FOR STABILITY AND DYNAMIC RESPONSE ANALYSIS OF RAIL VEHICLE SYSTEMS, Volume I: Technical Report

5. Report Date
February 1975

6. Performing Organization Code

7. Author(s)
T. K. Hasselman, Allen Brousowicki, Gary C. Hart

8. Performing Organization Report No.
DOT-TSC-FRA-74-14.I

9. Performing Organization Name and Address
J. H. Wiggins Company
1650 South Pacific Coast Highway
Redondo Beach CA 90277

10. Work Unit No. (TRAIS)
RR415/R5301

11. Contract or Grant No.
DOT-TSC-760-1

12. Sponsoring Agency Name and Address
U.S. Department of Transportation
Federal Railroad Administration
Office of Research and Development
Washington DC 20590

13. Type of Report and Period Covered
Final Report
26 Feb. 1974-3 Oct. 1974

14. Sponsoring Agency Code

15. Supplementary Notes
This work was performed under Contract No. DOT-TSC-760 for the U. S. Department of Transportation, Transportation Systems Center, Kendall Square, Cambridge MA 02142 .

16. Abstract

A methodology and a computer program, DYNALIST II, have been developed for computing the response of rail vehicle systems to sinusoidal or stationary random rail irregularities. The computer program represents an extension of the earlier DYNALIST program A modal synthesis procedure is used which permits the modeling of subsystems or components by partial modal representation using complex eigenvectors. Complex eigenvectors represent the amplitude and phase characteristics of rail vehicle systems which occur as a result of wheel-rail interaction, heavy damping in the suspension system and rotating machinery. Both vertical and lateral motion are handled by the program which allows up to twenty-five component and fifty system degrees of freedom.

17. Key Words	18. Distribution Statement
Rail Vehicle Dynamics, Rail Vehicle Stability, Rail Vehicle Response, Ride Quality, Computer Modeling, Modal Synthesis	DOCUMENT IS AVAILABLE TO THE PUBLIC THROUGH THE NATIONAL TECHNICAL INFORMATION SERVICE, SPRINGFIELD, VIRGINIA 22161

19. Security Classif. (of this report)	20. Security Classif. (of this page)	21. No. of Pages	22. Price
Unclassified	Unclassified	118	5.50

Form DOT F 1700.7 (8-72)

PRICES SUBJECT TO CHANGE

* U. S. GOVERNMENT PRINTING OFFICE : 1973 729-904/330

PREFACE

The Federal Railroad Administration (FRA) is sponsoring research, development, and demonstration programs to provide improved safety, performance, speed, reliability, and maintainability of rail transportation systems at reduced life-cycle costs. A major portion of these efforts is related to improvement of the dynamic characteristics of rail vehicles, track structures, and train consists.

Transportation Systems Center (TSC) is maintaining a center for resources to be applied to programs for improved passenger service, improved safety, and more cost-effective freight service. As part of this effort, TSC is identifying computer programs, analytic models, and analysis tools required to support the FRA objectives. In particular, TSC is acquiring, developing, and extending computer programs to provide realistic predictions of rail system dynamic performance under field conditions.

The DYNALIST Program was initially developed for the Department of Transportation by TRW, Inc. to evaluate the stability of complex dynamic systems having up to 50 degrees of freedom. Under contract to TSC, in support of the FRA under PPA No. RR415, Dr. T.K. Hasselman of J.H. Wiggins Company extended the DYNALIST Program to provide a capability for predicting the response of rail vehicle/track systems to sinusoidal or stationary random rail irregularities. This report describes the results of that effort and is contained in two volumes. Volume I, the Technical Report, documents the theoretical basis of the program. Volume II, the User's Manual, describes use of the program and includes sample problems.

TABLE OF CONTENTS

LIST OF ILLUSTRATIONS

LIST OF ILLUSTRATIONS
(continued)

LIST OF ILLUSTRATIONS
(continued)

LIST OF TABLES

1. SUMMARY AND INTRODUCTION

1.1 Summary

This report presents results of research and computer program development on rail vehicle dynamics performed at the J. H. Wiggins Company during the period February, 1974 to October, 1974. The work covers the following major areas:

- Development of detailed equations for calculating acceleration, velocity, and displacement response at selected locations on a rail vehicle due to sinusoidal and/or stationary random track irregularities.
- Development of Fortran response code and plotting subroutines which implement the above methodology.
- Execution of sample problems to demonstrate use of the computer program for rail vehicle systems.

1.2 Introduction

The subject of rail vehicle response to guideway irregularities has been of interest to engineers for many years. These irregularities cause vibratory motion to be induced in the cars and their suspension systems. As a result, the passenger environment may become uncomfortable, wheels and rails wear more rapidly and in extreme cases, derailment may occur. All of these problems become more severe as vehicle speeds increase. For conventional wheel type suspension systems, the problems are compounded because the increase in speed is accompanied by the development of a self excited instability called hunting.

The dynamic behavior of conventional rail vehicles is unique among many dynamic systems due to the mechanics of wheel-rail interaction. Wheels are connected rigidly to the axles and given a slightly conical geometry so that they tend to "track" without wearing the flanges against the rails. The design gives rise to the potentially unstable hunting motion. This consideration, along with the large amounts of damping found in suspension systems, demands special modeling capabilities not commonly available. The important dynamic characteristics are still obtained by solving an eigenvalue problem, but the eigenvalues and eigenvectors are complex, as opposed to being real in the classical case. Complex eigenproblem solvers are generally available but input matrices must be generated by hand, a rather time-consuming task whenever the system contains more than 10 or 15 degrees of freedom. Furthermore, computer costs become excessive for larger systems, particularly when parametric studies are made.

Recognizing these limitations, the U. S. Department of Transportation sponsored the development of a general computer code for the modeling and analysis of rail vehicles systems. The methodology was formulated in 1970 and an operational program was delivered to DOT. Documentation is provided in Reference [1]*. This program was updated in 1973 and given the name DYNALIST (Dynamics of Articulated Linear Systems). The DYNALIST program utilizes a subsystems approach to generate complex eigenvalue and eigenvector characteristics of rail vehicle systems with up to 50 degrees of freedom.

This report concerns an extension of DYNALIST to enable computation of vehicle response to sinusoidal and stationary random rail irregularities. The new version of the program, called DYNALIST II, includes capabilities for stability as

* Numbers in square brackets designate references listed at the end of this report.

well as dynamic response analysis based on modal methods. CalComp plots of vehicle excitation and response characteristics versus frequency can be generated. Several improvements in the original part of the program have also been made to facilitate user convenience and extend the range of applicability to practical problems. Of particular importance are:

- A new capability for direct modal representation of flexible components such as car bodies. Component equations of motion may be written in terms of modal coordinates and subsequently transformed back to the physical coordinate system for response computation.
- Automatic generation of the IARANG vector used to distinguish between dependent and independent coordinates and establish the order of system coordinates.

The DYNALIST II computer program begins by generating a list of dynamic characteristics for each subsystem or component treated independently. The list may then be edited to delete characteristics associated with large eigenvalues. Then component data are assembled from the list to form the equations of motion for the composite system and solved in a reduced coordinate space. The program represents a generalization of the usual component mode synthesis method used in structural dynamics. DYNALIST II will accommodate systems subdivided into components having up to twenty-five degrees of freedom each. Flexible truck assemblies and car bodies may be treated as individual components. Only one component of a kind need be placed on the master component list. The list can be saved on a permanent file or tape and added to at any time. In this way a variety of building blocks can be stored and combined in different ways to synthesize a variety of rail vehicle systems.

Changing truck assemblies, for example, to evaluate the effect on critical speed or ride quality is a simple matter since the user need only change the component names on the assembly list, a subset of the master list.

After assembling the system from the list of components on file, the program generates the complex modal characteristics of the system which may be written onto a permanent file or tape. A user option provides for termination of the program at this point, or continuation to the response segment. A restart capability is provided.

In the response segment of the program the complex frequency response at selected vehicle locations is generated using the complex modal characteristics previously obtained. The user then has the option to specify either sinusoidal or random input characteristics which define vehicle excitation. The phasing of inputs at each axle is computed on the basis of user input lag terms which depend on axle spacing and velocity. Depending on the form of excitation specified, sinusoidal response or random response is computed and plotted versus frequency. Random response is computed in the form of a power spectral density function dependent on frequency. Mean-square values of response are also computed by integrating the response PSD functions.

The DYNALIST II program offers the user considerable flexibility in computational methods as well as modeling ability. The following options are available:

- Direct System Method - System is modeled as a single component. Complex modes are evaluated directly and may be truncated for response computation.
- Direct Subsystems Method - System is modeled as an assembly of subsystems. However, no subsystem modes are computed. System modes are computed directly and may be truncated for response computation.

- Modal Synthesis Method - System is modeled as an assembly of subsystems. Subsystem or component modes are generated and these may be truncated prior to assembling the system. System modes are then generated and these also may be truncated for response computation.

The remaining chapters of this report describe in detail the methods of analysis and the example problems which have been evaluated.

2. THEORETICAL DEVELOPMENT

A formal presentation of the modal synthesis procedure is described in this chapter. Coordinate transformations are defined using complex modal matrices. The response of the system to rail irregularities is developed using the frequency response method.

2.1 Discussion of Coordinate Systems

Prior to the derivation of detailed equations which form the computational basis of DYNALIST II, it will be useful to discuss the relationship among the various coordinate systems involved. This will serve to introduce some of the notation as well as provide a general overview of analytical procedures.

Six different coordinate systems are used in all. Three of these define displacements of the system at either the component or the system level. The remaining three are state space coordinate systems which include both velocity and displacement. The use of state space coordinates is a direct consequence of reducing the second order differential equations of motion to first order form. This step is taken to extract the complex eigenvalues and eigenvectors which are characteristic of rail vehicle components and systems.

There are two kinds of components which form the building blocks used to generate DYNALIST models: structural components such as car bodies and truck frames, whose dynamic characteristics (eigenvalues and eigenvectors) are real and classical in form; and the complementary group of all other components such as truck assemblies and cars which include suspension elements and rotating machinery. The dynamic characteristics of these components are considered to be complex. The latter group of components may include some of the former as elements, e.g., a car

component in a train may include a flexible car body. The distinction is important with regard to understanding the input coordinate system, i.e., the coordinate system in which component equations of motion are initially specified.

The six coordinate systems will be denoted by the vectors u, p, q, x, y, and z. Input is specified in the p coordinate system. In the case of nonrigid structural components, the equations of motion will be written in modal coordinates. In this way, a car body, for example, may be represented by its flexural modes. However, when response is computed, transformation back to the physical coordinate system, u, is required to facilitate interpretation. Therefore, the modal transformation matrix ϕ must also be supplied.

When modeling the more general class of components, equations of motion may be written in terms of discrete coordinates, distributed coordinates, or a combination of the two. When certain p coordinates correspond to physical displacements, the modal matrix ϕ must embody the appropriate identity relationships. Corresponding elements in the u coordinate system will, therefore, have the same meaning.

The component equations of motion are coupled by introducing equations of constraint which lead to a compatibility matrix $\overline{\beta}$ relating the component coordinates p to a set of generalized coordinates q for the complete system. The q coordinates are defined so as to preserve all of the original component coordinates which are not on interface boundaries. Then by fixing the interface boundaries, constrained component modes are computed for the individual components, e.g., single cars of a train. This leads to the second modal transformation designated by $\overline{\Psi}$ which transforms the coordinates from q, through

an intermediate vector x which contains both q and $\dot{q}$, to y. The matrix $\overline{\Psi}$ is complex in general. The purpose of this transformation is to further reduce the number of coordinates required to describe the system by permitting truncation of the complex component modes. Finally, the reduced set of system equations is considered in homogenous form to generate a set of system modes Ψ_y which is used to transform the system state equations in coordinates y to diagonal form in coordinates z. This then is the third modal transformation.

Frequency response functions are computed in the z coordinate system and transformed back through the sequence of previously defined transformations to the set of u coordinates which are identified with discrete points on the system.

2.2 Formulation of Component Equations

The method described herein and implemented in the DYNALIST II computer program is not intended for use in solving real eigenproblems, although real eigenproblems can be solved using the complex eigenproblem subroutines contained therein. However, this is not the intent and would be quite inefficient. There are many cases in which the user will want to include flexible structural components in his model. As previously stated, the component equations of motion are entered in terms of the real component mode coordinates, p, and in addition, the real component mode transformations ϕ are entered as input to the program.

In specifying the constraint equations which establish component displacement compatibility, it is convenient to do so in the discrete physical coordinate system, u, rather than the modal coordinates, p. Therefore, constraint equations of the form

$$[G]\ \{u\} = \{0\} \quad \ldots\ldots\ldots\ldots \quad (2\text{-}1)$$

are defined and the matrix ϕ is used to determine the corresponding set of equations

$$[G]\ [\phi]\ \{p\} = \{0\} \quad . \quad . \quad . \quad . \quad . \quad . \quad . \quad . \quad (2\text{-}2)$$

It may be pointed out here that the column vectors, ϕ_j, which comprise ϕ need not be complete. Of course, the number of columns in ϕ will correspond to the number of component mode coordinates reflected in the vector p which will in general be equal to or less than the total number of degrees of freedom in the physical coordinate system. The point stressed here, however, is that the vector u need not contain all of the physical coordinates so that ϕ will have a partial set of rows as well as a partial set of columns.

What determines the columns and rows to be included in ϕ? Clearly, the columns in ϕ will correspond to the rigid body, constraint, and low-order dynamic (normal) modes for the various components. Three factors determine the particular rows to be included. First, the rows corresponding to elements of u involved in the constraint equation (2-1) must be included. Second, the rows corresponding to the elements of u for which response is desired must be included. Third, rows corresponding to elements of u at which external forces (including wheel-rail forces) are applied must be included.

For example, consider the train car having a flexible car body as shown in Figure 2-1. The car body has four modal coordinates describing its motion: two rigid body modes, p_1^2 and p_2^2 and two flexible body modes p_3^2 and p_4^2.

Seven discrete coordinates, u_1^2 through u_7^2 are also defined. Coordinates u_1^2 through u_4^2 will be used in the constraint

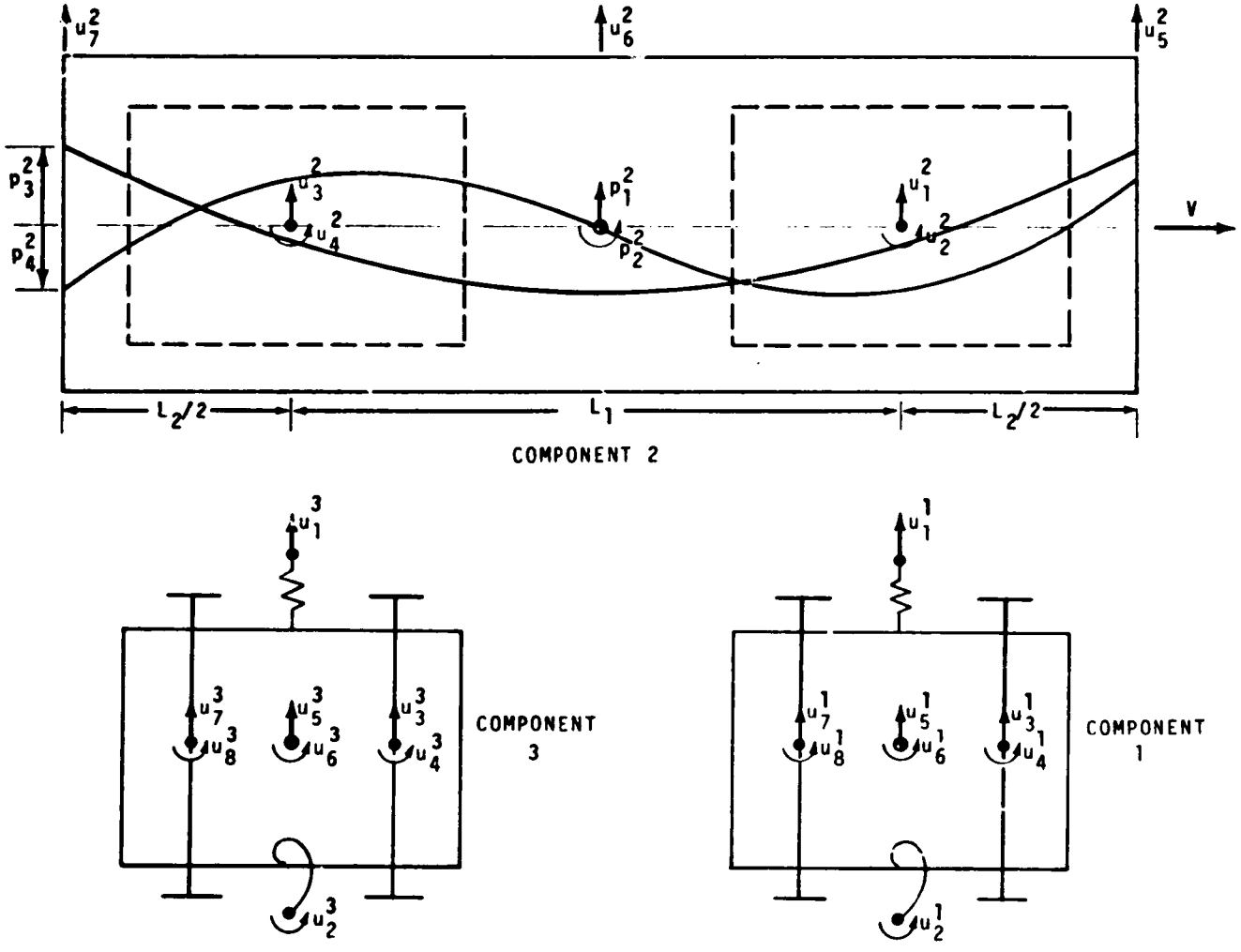

Figure 2-1 Train Car with Flexible Car Body

equations while u_5^2 through u_7^2 are defined for response computation. In other words, lateral response will be computed at both ends and at the center of the car.

The real mode transformations for each of the components are as follows:

Component 1

$$\begin{Bmatrix} u_1^1 \\ u_2^1 \\ u_3^1 \\ u_4^1 \\ u_5^1 \\ u_6^1 \\ u_7^1 \\ u_8^1 \end{Bmatrix} = \overbrace{\begin{bmatrix} 1 & & & & & & & \\ & 1 & & & & & & \\ & & 1 & & & & & \\ & & & 1 & & & & \\ & & & & 1 & & & \\ & & & & & 1 & & \\ & & & & & & 1 & \\ & & & & & & & 1 \end{bmatrix}}^{\phi^{1C}\quad \phi^{1F}} \begin{Bmatrix} p_1^1 \\ p_2^1 \\ p_3^1 \\ p_4^1 \\ p_5^1 \\ p_6^1 \\ p_7^1 \\ p_8^1 \end{Bmatrix} \begin{matrix} \} p^{1C} \\ \} p^{1F} \end{matrix}$$

Component 2

$$\begin{Bmatrix} u_1^2 \\ u_2^2 \\ u_3^2 \\ u_4^2 \\ u_5^2 \\ u_6^2 \\ u_7^2 \end{Bmatrix} = \overbrace{\begin{bmatrix} 1 & L_1/2 & \phi_{11}^C & \phi_{12}^C \\ 0 & 1 & \phi_{21}^C & \phi_{22}^C \\ 1 & -L_1/2 & \phi_{31}^C & \phi_{32}^C \\ 0 & 1 & \phi_{41}^C & \phi_{42}^C \\ 1 & (L_1 + L_2)/2 & \phi_{51}^C & \phi_{52}^C \\ 1 & 0 & \phi_{61}^C & \phi_{62}^C \\ 1 & -(L_1 + L_2)/2 & \phi_{71}^C & \phi_{72}^C \end{bmatrix}}^{\phi^{2R}\quad \phi^{2C}} \begin{Bmatrix} p_1^2 \\ p_2^2 \\ p_3^2 \\ p_4^2 \end{Bmatrix} \begin{matrix} \} p^{2R} \\ \} p^{2C} \end{matrix}$$

Component 3

$$\begin{Bmatrix} u_1^3 \\ u_2^3 \\ u_3^3 \\ u_4^3 \\ u_5^3 \\ u_6^3 \\ u_7^3 \\ u_8^3 \end{Bmatrix} = \begin{bmatrix} \overbrace{1 & & \\ & 1 & \\ & & 1}^{\phi^{3C}} & \overbrace{\begin{matrix} & & & & \\ 1 & & & & \\ & 1 & & & \\ & & 1 & & \\ & & & 1 & \\ & & & & 1 \end{matrix}}^{\phi^{3F}} \end{bmatrix} \begin{Bmatrix} p_1^3 \\ p_2^3 \\ p_3^3 \\ p_4^3 \\ p_5^3 \\ p_6^3 \\ p_7^3 \\ p_8^3 \end{Bmatrix} \begin{matrix} \} p^{3C} \\ \\ \\ \} p^{3F} \end{matrix}$$

All of these equations are of the form

$$u^{\ell} = \phi^{\ell} p^{\ell} \quad \ldots\ldots\ldots\ldots \quad (2\text{-}3)$$

It is emphasized that the vector p^{ℓ} must be arranged so that

$$p^{\ell} = \begin{Bmatrix} p^{\ell R} \\ \hline p^{\ell C} \\ \hline p^{\ell F} \end{Bmatrix} \quad \ldots\ldots\ldots\ldots \quad (2\text{-}4)$$

where $p^{\ell R}$ is a vector containing a component's rigid body degrees of freedom, $p^{\ell C}$ contains the constraint degrees of freedom and $p^{\ell F}$ contains the free coordinates. The distinction between rigid body and constraint, and free coordinates is quite essential to the proper execution of DYNALIST II. The solution of the component eigenproblem involves only the free coordinates. It may be noted that the ϕ^2 matrix for component 2 contains no ϕ^{2F} columns and the real normal mode vectors are included in ϕ^{2C} instead. This is because the computer program

makes a test to determine whether the number of free coordinates, NFREE, is greater than zero. If NFREE is greater than zero, a complex eigenproblem is formulated and solved for that component. Since complex modes are not required for the car-body component in the above example, NFREE must equal zero.

It is not necessary to distinguish between ϕ^R and ϕ^C. Both could be lumped in a matrix called ϕ^B as is done in [2]. There is one subtle factor which will emerge later. In defining the compatibility transformation, the independent coordinates must provide a basis for the dependent coordinates. It is thus helpful to keep clear which coordinates are rigid-body, constraint and free.

The equations of motion for the ℓth component in the physical u coordinate system are considered to be of the form

$$\mu^\ell \ddot{u}^\ell + \gamma^\ell \dot{u}^\ell + \kappa^\ell u^\ell = f_u^\ell (t) \quad \ldots\ldots\ldots\ldots \quad (2\text{-}5)$$

Introducing a real modal transformation to simplify the modeling of flexible structural elements or components results in

$$u^\ell = \phi^\ell p^\ell \quad \ldots\ldots\ldots\ldots\ldots\ldots \quad (2\text{-}6)$$

Under this transformation, (2-5) becomes

$$\phi^{\ell T} \mu^\ell \phi^\ell \ddot{p}^\ell + \phi^{\ell T} \gamma^\ell \phi^\ell \dot{p}^\ell + \phi^{\ell T} \kappa^\ell \phi^\ell p^\ell = \phi^{\ell T} f_u^\ell = f_p^\ell$$

or alternatively

$$m^\ell \ddot{p}^\ell + c \dot{p}^\ell + k^\ell p^\ell = f_p^\ell \quad \ldots\ldots\ldots\ldots \quad (2\text{-}7)$$

Component equations of motion are input to DYNALIST II by specifying the matrices m^ℓ, c^ℓ and k^ℓ in the p-coordinate system.

Forces are specified in the u-coordinate system, however, because it is more convenient to enter forces in the physical coordinate system and let the computer make the transformation, $f_p = \phi^T f_u$.

Now the complex eigenproblem for each component may be considered. Equation (2-7) may be partitioned so as to separate the rigid body, p^R, constraint, p^C, and free, p^F, coordinates in the manner

$$\begin{bmatrix} m^{RR} & m^{RC} & m^{RF} \\ m^{CR} & m^{CC} & m^{CF} \\ m^{FR} & m^{FC} & m^{FF} \end{bmatrix}^{\ell} \begin{Bmatrix} \ddot{p}^R \\ \ddot{p}^C \\ \ddot{p}^F \end{Bmatrix}^{\ell} + \begin{bmatrix} c^{RR} & c^{RC} & c^{RF} \\ c^{CR} & c^{CC} & c^{CF} \\ c^{FR} & c^{FC} & c^{FF} \end{bmatrix}^{\ell} \begin{Bmatrix} \dot{p}^R \\ \dot{p}^C \\ \dot{p}^F \end{Bmatrix}$$

$$+ \begin{bmatrix} k^{RR} & k^{RC} & k^{RF} \\ k^{CR} & k^{CC} & k^{CF} \\ k^{FR} & k^{FC} & k^{FF} \end{bmatrix}^{\ell} \begin{Bmatrix} p^R \\ p^C \\ p^F \end{Bmatrix}^{\ell} = \begin{Bmatrix} f_p^R \\ f_p^C \\ f_p^F \end{Bmatrix}^{\ell} \quad \ldots\ldots \text{(2-8)}$$

The constrained component eigenproblem is obtained by assuming the $p^{\ell R}$ and $p^{\ell C}$ coordinates to be fixed, in which case the homogeneous form of (2-8) becomes

$$m^{\ell FF}\, \ddot{p}^{\ell F} + c^{\ell FF}\, \dot{p}^{\ell F} + k^{\ell FF}\, p^{\ell F} = 0 \quad \ldots\ldots\ldots \text{(2-9)}$$

The corresponding first order equations are

$$\begin{bmatrix} c^{FF} & m^{FF} \\ m^{FF} & 0 \end{bmatrix}^{\ell} \begin{Bmatrix} \dot{p}^F \\ \ddot{p}^F \end{Bmatrix}^{\ell} + \begin{bmatrix} k^{FF} & 0 \\ 0 & -m^{FF} \end{bmatrix}^{\ell} \begin{Bmatrix} p^F \\ \dot{p}^F \end{Bmatrix}^{\ell} = \begin{Bmatrix} 0 \\ 0 \end{Bmatrix} \quad \ldots \text{(2-10)}$$

and the corresponding eigenproblem is

$$\left(\left[\begin{array}{c|c} c^{FF} & m^{FF} \\ \hline m^{FF} & 0 \end{array} \right]^{\ell} \lambda_j^{\ell} + \left[\begin{array}{c|c} k^{FF} & 0 \\ \hline 0 & -m^{F\bar{F}} \end{array} \right]^{\ell} \right) \left\{ \psi_j \right\}^{\ell} = \left\{ \begin{array}{c} 0 \\ \hline 0 \end{array} \right\} \quad \ldots \quad (2\text{-}11)$$

where λ_j^{ℓ} and $\{\psi_j\}^{\ell}$ are the complex eigenvalues and eigenvectors of the ℓth component. It is recognized that one may perform the partitioning

$$\left\{ \psi_j \right\}^{\ell} = \left\{ \begin{array}{c} \psi_{U_j} \\ \hline \psi_{L_j} \end{array} \right\} = \left\{ \begin{array}{c} \psi_{U_j}^{\ell} \\ \hline \psi_{U_j}^{\ell} \lambda^{\ell} \end{array} \right\} \quad \ldots \quad (2\text{-}12)$$

since solutions of the eigenvalue problem are of the form

$$p^{\ell F} = \psi_{U_j}^{\ell} e^{\lambda_j^{\ell} t} \quad \ldots \quad (2\text{-}13)$$

The formulation and solution of the complex component eigenproblem was introduced here because it follows logically from the partitioning of Equation (2-8). However, we are not quite ready to use the results, ψ_j^{ℓ} and λ_j^{ℓ}. Furthermore, the constraint equations were introduced in (2-1) in order to help describe the component coordinates. The constraint equations must be used to derive a compatibility transformation to effect the mathematical coupling of component equations. It is desirable that this be done prior to making the complex component mode transformations in order to perform the operations in real arithmetic. The following two sections will therefore consider first the compatibility transformation, and then complex modal synthesis where the component "free" coordinates are transformed to complex modal coordinates.

2.3 Compatibility Relationships Between Components

Going back to (2-7) one may form a set of equations for the system in block diagonal form where the coupling between components is implicit in the forces on the right-hand side. Thus

$$\begin{bmatrix} m^1 & & & \\ & m^2 & & \\ & & \ddots & \\ & & & m^N \end{bmatrix} \begin{Bmatrix} \ddot{p}^1 \\ \ddot{p}^2 \\ \vdots \\ \ddot{p}^N \end{Bmatrix} + \begin{bmatrix} c^1 & & & \\ & c^2 & & \\ & & \ddots & \\ & & & c^N \end{bmatrix} \begin{Bmatrix} \dot{p}^1 \\ \dot{p}^2 \\ \vdots \\ \dot{p}^N \end{Bmatrix} + \begin{bmatrix} k^1 & & & \\ & k^2 & & \\ & & \ddots & \\ & & & k^N \end{bmatrix} \begin{Bmatrix} p^1 \\ p^2 \\ \vdots \\ p^N \end{Bmatrix}$$

$$= \begin{Bmatrix} f_p^1 \\ f_p^2 \\ \vdots \\ f_p^N \end{Bmatrix}$$

where N = number of components in the system. Alternatively,

$$m\ddot{p} + c\dot{p} + kp = f_p \quad \ldots\ldots\ldots\ldots\ldots\ldots \quad (2\text{-}14)$$

Constraint equations in the general form

$$[G]\{u\} = \{0\} \quad \ldots\ldots\ldots\ldots\ldots\ldots \quad (2\text{-}1)$$

have been written where it is now recognized that

$$\{u\} = \begin{Bmatrix} u^1 \\ u^2 \\ \vdots \\ u^N \end{Bmatrix} \quad \ldots\ldots\ldots\ldots\ldots\ldots \quad (2\text{-}15)$$

Transformation to the p coordinate system has been written as

$$[G][\phi]\{p\} = \{0\} \quad \ldots\ldots\ldots\ldots\ldots\ldots \quad (2\text{-}2)$$

where

$$[\phi] = \begin{bmatrix} \phi^1 & & & \\ & \phi^2 & & \\ & & \ddots & \\ & & & \phi^N \end{bmatrix} \quad \ldots\ldots\ldots\ldots\ldots \quad (2\text{-}16)$$

Finally, the redundant coordinates in the vector p must be eliminated by the compatibility constraint equations. Let the reordering matrix E partition p so that the dependent coordinates, $\bar{p}_d$, appear first, followed by those which are independent (free) $\bar{p}_f$.[+] Thus,

$$\{p\} = [E]\{\bar{p}\} = [E]\begin{Bmatrix} \bar{p}_d \\ \hline \bar{p}_f \end{Bmatrix} \quad \ldots\ldots\ldots\ldots\ldots (2\text{-}17)$$

and then (2-16) becomes

$$[G][\phi][E]\{\bar{p}\} = [\bar{G}]\{\bar{p}\} = \{0\} \quad \ldots\ldots\ldots\ldots (2\text{-}18)$$

$$[\bar{G}_d \mid \bar{G}_f]\begin{Bmatrix} \bar{p}_d \\ \hline \bar{p}_f \end{Bmatrix} = \{0\} \quad (2\text{-}19)$$

$$\{\bar{p}_d\} = -[\bar{G}_d]^{-1}[\bar{G}_f]\{\bar{p}_f\} = [\beta]\{\bar{p}_f\} \quad \ldots\ldots\ldots (2\text{-}20)$$

$$\{p\} = [E]\{\bar{p}\} = [E]\begin{Bmatrix} \bar{p}_d \\ \hline \bar{p}_f \end{Bmatrix} = [E]\begin{bmatrix} -\beta \\ \hline I \end{bmatrix}\{\bar{p}_f\} = [\bar{\beta}]\{q\} \quad \ldots\ldots (2\text{-}21)$$

where q denotes the <u>generalized coordinates</u> of the system.

Going back to the system of Figure 2-1 to give these transformations physical meaning, one may write the system u and p coordinates as

---

[+]The subscript, f, used here is not to be confused with the superscript, F, used in (2-8). The latter denotes component coordinates for which complex component modes are to be computed. The former denotes all independent coordinates for the entire system. These include all of the "F" as well as some of the "R" and "C" coordinates.

$$\{u\} = \begin{Bmatrix} u^1 \\ u^2 \\ u^3 \end{Bmatrix} = \{u_1^1, u_2^1, \ldots, u_8^1, u_1^2, u_2^2, \ldots, u_7^2, u_1^3, u_2^3, \ldots, u_8^3\}^T \quad \ldots (2\text{-}22)$$

$$\{p\} = \begin{Bmatrix} p^1 \\ p^2 \\ p^3 \end{Bmatrix} = \{p_1^1, p_2^1, \ldots, p_8^1, p_1^2, p_2^2, p_3^2, p_4^2, p_1^3, p_2^3, \ldots, p_8^3\}^T \quad \ldots (2\text{-}23)$$

The constraint matrix, G, of Equation (2-15) connects the three sets of coordinates in the physical, u, coordinate system. Thus coordinates u_1^1 and u_2^1 of component 1 are constrained to move with coordinates u_1^2 and u_2^2. Similarly, u_1^3 and u_2^3 move with u_3^2 and u_4^2. Equation (2-15) may then be written

$$[G]\{u\} = \left[\begin{array}{cccccccc|cccccccc|cccccccc} 1&0&0&0&0&0&0&0&-1&0&0&0&0&0&0&0&0&0&0&0&0&0&0&0 \\ 0&1&0&0&0&0&0&0&0&-1&0&0&0&0&0&0&0&0&0&0&0&0&0&0 \\ 0&0&0&0&0&0&0&0&0&0&-1&0&0&0&0&1&0&0&0&0&0&0&0&0 \\ 0&0&0&0&0&0&0&0&0&0&0&-1&0&0&0&0&1&0&0&0&0&0&0&0 \end{array}\right] \{u\} = \{0\} \quad \ldots (2\text{-}24)$$

Equation (2-24) contains four rows since there are four physical constraints. The constraints are converted to the p-system through (2-16) and then four p-coordinates $\bar{p}_d$, are eliminated through (2-20). It is first necessary, however, to choose which dependent coordinates to eliminate. One must input this information to DYNALIST II in the vector KDEP, which contains the numbers of the dependent p-coordinates. This information is then used to automatically generate the matrix E of (2-17). The only restriction on defining KDEP is that the submatrix $[\bar{G}_d]$ in (2-19) be nonsingular since it must be inverted to generate the compatibility transformation, $[\bar{\beta}]$. For n equations of constraint, the first n columns of $\bar{G}$ must be linearly independent.

In order to generate the system equations of motion, the transformation (2-21) applied to (2-14) yields

$$\bar{\beta}^T m \bar{\beta} \ddot{q} + \bar{\beta}^T c \bar{\beta} \dot{q} + \bar{\beta}^T k \bar{\beta} q = \bar{\beta}^T f_p = f_q$$

or alternatively

$$M\ddot{q} + C\dot{q} + Kq = f_q \quad \cdots\cdots\cdots\cdots\cdots \quad (2\text{-}25)$$

Equation (2-25) represents the system dynamical equations of motion. A direct numerical solution to this equation is possible. However, experience with the solution to equations of this type indicates that when using modal synthesis methods one gains economic efficiency as well as engineering insight. The pages which follow discuss the modal synthesis technique used in DYNALIST II.

2.4 Complex Modal Synthesis

It is recalled from (2-11), from which the complex component modes are calculated, that it is possible to make the following coordinate transformation,

$$\begin{Bmatrix} p^F \\ \dot{p}^F \end{Bmatrix}^{\ell} = \begin{bmatrix} \psi_U^{\ell} \\ \hline \psi_U^{\ell} \lambda \end{bmatrix} \{\eta\}^{\ell} \quad \cdots\cdots\cdots\cdots \quad (2\text{-}26)$$

These transformations may be combined to give

$$\{q^F\} = \{p^F\} = \begin{Bmatrix} p^{1F} \\ p^{2F} \\ \vdots \\ p^{NF} \end{Bmatrix} = \begin{bmatrix} \psi_U^1 & & & \\ & \psi_U^2 & & \\ & & \ddots & \\ & & & \psi_U^N \end{bmatrix} \{\eta\} = [\psi_U]\{\eta\}$$

and $\{\dot{q}^F\} = \{\dot{p}^F\} = [\psi_U][\lambda]\{\eta\}$ so that

$$x = \begin{Bmatrix} q \\ \dot{q} \end{Bmatrix} = \begin{Bmatrix} q^{RC} \\ q^{F} \\ \dot{q}^{RC} \\ \dot{q}^{F} \end{Bmatrix}^{\dagger} = \begin{bmatrix} I & 0 & 0 \\ 0 & 0 & \psi_U \\ 0 & I & 0 \\ 0 & 0 & \psi_U\lambda \end{bmatrix} \begin{Bmatrix} q^{RC} \\ \dot{q}^{RC} \\ \eta \end{Bmatrix} = [\bar{\psi}]\{y\} \quad \ldots\ldots (2\text{-}27)$$

Equation (2-25) written in first order form is

$$\begin{bmatrix} C & M \\ M & 0 \end{bmatrix} \begin{Bmatrix} \dot{q} \\ \ddot{q} \end{Bmatrix} + \begin{bmatrix} K & 0 \\ 0 & -M \end{bmatrix} \begin{Bmatrix} q \\ \dot{q} \end{Bmatrix} = \begin{Bmatrix} f_q \\ 0 \end{Bmatrix}$$

or alternatively,

$$A_x\dot{x} + B_x x = f_x \quad \ldots\ldots\ldots\ldots\ldots\ldots (2\text{-}28)$$

Introducing the coordinate transformation defined in (2-27) to (2-28) yields

$$\bar{\psi}^T A_x \bar{\psi}\dot{y} + \bar{\psi}^T B_x \bar{\psi} y = \bar{\psi}^T f_x = f_y$$

or alternatively,

$$A_y\dot{y} + B_y y = f_y \quad \ldots\ldots\ldots\ldots\ldots\ldots (2\text{-}29)$$

The final system eigenproblem may now be written

$$(A_y\Lambda_j + B_y)\Psi_{y_j} = 0 \quad \ldots\ldots\ldots\ldots\ldots\ldots (2\text{-}30)$$

whereupon the additional coordinate transformation

$$y = \Psi_y z \quad \ldots\ldots\ldots\ldots\ldots\ldots\ldots\ldots (2\text{-}31)$$

applied to (2-29) results in

†The superscript "RC" is used here to denote those rigid body and constraint coordinates which were not eliminated by constraint equations, i.e., they are a subset of the vector "$\bar{p}_f$" defined in (2-17).

$$\dot{z} - \Lambda z = A_z^{-1} \psi_y^T f_y = A_z^{-1} f_z \quad \ldots\ldots\ldots\ldots (2\text{-}32)$$

Equation (2-32) represents the system dynamical equations of motion in terms of first order system normal modes of vibration. The matrix transformations from the complex system mode coordinates back to the physical coordinate system follow directly from the application of (2-31), (2-27), (2-21) and (2-6). Thus it is found that

$$\{u\} = [\phi][\bar{\beta}][\bar{\psi}_U][\psi_y]\{z\} \quad \ldots\ldots\ldots\ldots (2\text{-}33)$$

The differential equations of motion given in (2-32) can be solved for any specified form of forcing function. In the sections which follow the excitation is considered to be induced by rail irregularities. The analytical form of these irregularities is assumed to be either sinusoidal or stationary random. In either case the solution is dependent upon the system's frequency response function.

2.5 Frequency Response to Rail Irregularities

The frequency response function for a linear system is defined to be the complex ratio of output over input as a function of the input frequency. For example, an equation of motion for a single degree of freedom system may be written

$$m\ddot{x}(t) + c\dot{x}(t) + kx(t) = f(t)$$

Transformation to the frequency domain, Ω, results in

$$[(k-\Omega^2 m) + i\Omega c]\, X(i\Omega) = F(i\Omega)$$

The complex frequency response function is defined to be

$$H_x(i\Omega) \equiv \frac{X(i\Omega)}{F(i\Omega)} = \frac{1}{(k-\Omega^2 m)+i\Omega c}$$

It is a characteristic of the system and is independent of applied forces.

For a base excited system, where a mass is attached to some movable base by a spring, k, and a dashpot, c, the equation of motion is

$$m\ddot{x} + c(\dot{x}-\dot{x}_b) + k(x-x_b) = 0$$

or

$$m\ddot{x} + c\dot{x} + kx = c\dot{x}_b + kx_b$$

In this case, transformation to the frequency domain yields

$$[(k-\Omega^2 m) + i\Omega c]\, X(i\Omega) = (k+i\Omega c)X_b(i\Omega)$$

Defining the frequency response function as before such that $H_x(i\Omega) = X(i\Omega)/X_b(i\Omega)$, one obtains

$$[(k-\Omega^2 m) + i\Omega c]\, H_x(i\Omega) = k + i\Omega c$$

The right hand side of the above equation may be written in the general form

$$k + (i\Omega)c = F_o + (i\Omega)F_1 + (i\Omega)^2 F_2$$

where in this case, $F_2 = 0$.

For a multi degree-of-freedom base excited system, the general form of the equations of motion transformed to the frequency domain may be written

$$([k] - \Omega^2[m]+i\Omega[c])\{H_x(i\Omega)\} = \{F_o\} + i\Omega\{F_1\} + (i\Omega)^2\{F_2\}$$

where $H_x(i\Omega)$ denotes the complex frequency response vector, [k], [m] and [c] are square matrices and $\{F_j\}$, $j = 0,1,2$ is a vector. It has been assumed that vector of applied forces is of the form $\{F\}X_b(i\Omega)$ so that

$$\{F\} = \{F_o\} + i\Omega\{F_1\} + (i\Omega)^2\{F_2\}$$

and

$$\{H_x(i\Omega)\} = \frac{1}{X_b(i\Omega)} \{X(i\Omega)\}$$

where $X_b(i\Omega)$ is a scalar function. The vector $\{F\}$ is referred to as a spacial distribution vector while $x_b(t)$ is a scalar time dependent forcing function.

In the rail vehicle problem, the input is through the wheels. Since the irregularity traversed by one wheel is traversed by all other wheels at times which depend on wheel spacing, there is a phase relationship among the input forces. Thus, even if the vectors $\{F_1\}$ and $\{F_2\}$, above were both null, the distribution vector would be complex if the time dependent portion of the forcing function is considered to be a scalar function of time describing rail irregularity.

The equations of motion of a rigid wheelset are discussed in detail in Appendix A. Equation (A-16) and (A-19) show that in the case of lateral motion, the rail irregularities induce forces only at wheelset rotational coordinates. With regard to the previous discussion it becomes apparent that when the response of the rail vehicle system is calculated due to rail irregularities, only those coordinates corresponding to wheelset rotations will have non-zero force components. Referring to Figure 2-1, one sees that the only coordinates with non-zero forces are u_4^1, u_8^1, u_4^3 and u_8^3.

Consider the truck shown in Figure 2-2. Forces will be transmitted to the system corresponding to the u_2 and u_6 coordinates. It is apparent that if the vehicle is translating at a constant speed V and if the wheelsets are separated by a distance L, then

$\delta_1^{\ell}(t)$ = lateral displacement of rail at time t for the leading wheelset

and

$\delta_5^{\ell}(t)$ = lateral displacement of rail at time t for the trailing wheelset

are related by

$$\delta_5^{\ell}(t) = \delta_1^{\ell}(t - \frac{L}{V}) \quad \ldots\ldots\ldots\ldots\ldots \quad (2\text{-}34)$$

A meaningful relationship between these displacements follows after one takes the Laplace transform of (2-34), i.e.

$$\Delta_5^{\ell}(s) = \int_0^{\infty} \delta_5^{\ell}(t) e^{st} dt = e^{s(L/V)} \Delta_1^{\ell}(s). \quad \ldots\ldots \quad (2\text{-}35)$$

Replacing (s) by ($i\Omega$) yields the following frequency dependent relationship:

$$\Delta_5^{\ell}(i\Omega) = e^{i\Omega(L/V)} \Delta_1^{\ell}(i\Omega) \quad (2\text{-}36)$$

An important part of the response relationship for random irregularities is the complex frequency response between track irregularity and a response coordinate. The track irregularities provide input forces of the form given in (A-16) and (A-19), and appear in the $f_u^{\ell}(t)$ vector given in (2-5). The frequency representation of this force vector for the truck shown in Figure 2-2 takes the form

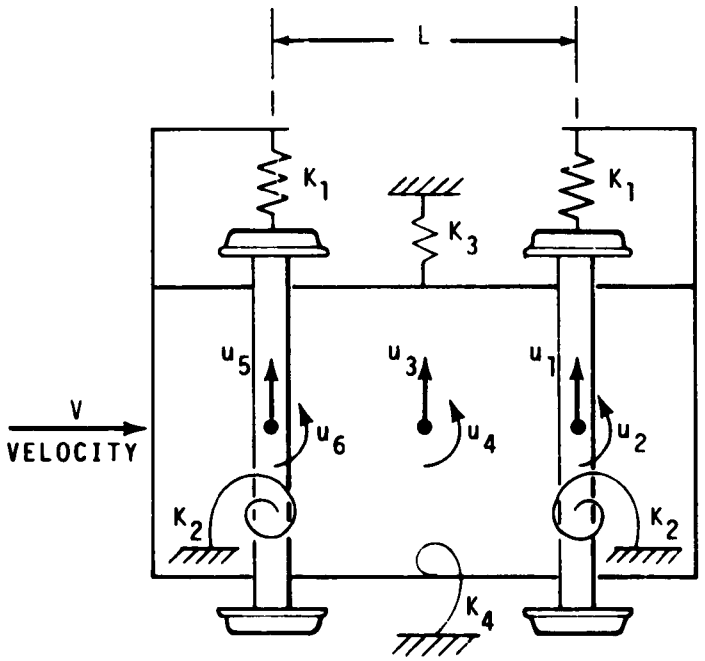

COMPONENT ℓ

Figure 2-2 Typical Truck System

$$\{F_u^{\ell}(i\Omega)\} = \begin{Bmatrix} 0 \\ \hline \left(\frac{2f\lambda_o L_o}{r_o}\right) \\ \hline 0 \\ \hline 0 \\ \hline \left(\frac{2f\lambda_o L_o}{r_o}\right) e^{i\Omega(L/V)} \end{Bmatrix} \Delta_1^{\ell}(i\Omega)$$

$$\left\{\bar{F}_u^{\ell}(i\Omega)\right\}\Delta_1^{\ell}(i\Omega) \quad \ldots\ldots\ldots\ldots \quad (2\text{-}37)$$

The complex force distribution vector including the phase shifts due to transportation lag may be written in the general form

$$\{\bar{F}(i\Omega)\} = \{\bar{F}_o(i\Omega)\} + i\Omega\{\bar{F}_1(i\Omega)\} + (i\Omega)^2\{\bar{F}_2(i\Omega)\} \quad (2\text{-}38)$$

where the subscripts denote zeroth, first and second order terms as before. The vector $\{\bar{F}_u^{\ell}(i\Omega)\}$ in Equation (2-37) corresponds to the $\{\bar{F}_o^{\ell}(i\Omega)\}$ term in (2-38).

The equations of motion given in Equation (2-32) may be transformed to the frequency domain resulting in

$$(i\Omega I - \Lambda) Z(i\Omega) = A_z^{-1} \bar{F}_z(i\Omega) \Delta_1^{\ell}(i\Omega) \quad \ldots\ldots\ldots (2\text{-}39)$$

or

$$(i\Omega I - \Lambda) H_z(i\Omega) = A_z^{-1} \bar{F}_z(i\Omega) \quad \ldots\ldots\ldots\ldots (2\text{-}40)$$

Rearranging (2-40) and using the transformations defined in previous sections one finds that

$$H_z(i\Omega) = [i\Omega I - \Lambda]^{-1} A_z^{-1} \psi_y^T \begin{Bmatrix} 0 \\ \hline 0 \\ \hline \psi_U^T \phi^T \bar{F}_u^F(i\Omega) \end{Bmatrix} \quad \ldots\ldots (2\text{-}41)$$

and the frequency response relationship in the u coordinate system is according to (2-33),

$$H_u(i\Omega) = \phi \bar{\beta}\, \bar{\psi}_U \psi_y H_z(i\Omega) \quad \ldots\ldots\ldots\ldots (2\text{-}42)$$

where

$$\bar{\psi}_U = \begin{bmatrix} I & 0 & 0 \\ 0 & 0 & \psi_U \end{bmatrix}$$

From (2-42) it follows that for any u_j coordinate one may write a corresponding

$H_{u_j}(i\Omega)$ = frequency response function relating rail irregularities and u_j coordinate response

The response of the vehicle system to sinusoidal or random rail irregularities involves the use of the system frequency response

function. Consideration will next be given to calculating vehicle response to such excitation.

2.6 Sinusoidal Rail Excitation

The evaluation of response to sinusoidal rail irregularities provides useful insight into the dynamic response characteristics of a rail vehicle system. While a more appropriate description of actual rail irregularities can be accomplished using a power spectral density function, it is important for two basic reasons to consider vehicle response to sinusoidal irregularities. Historically, rail irregularities have been described in terms of sinusoidal functions and, therefore, in order to relate to past work it is beneficial to consider sinusoidal excitations. Also, human comfort levels are most often prescribed in terms of sinusoidal environments and may, therefore, be compared directly to sinusoidal vehicle response.

The description of rail irregularities in sinusoidal terms involves relating the amplitude of the sine wave to its wave length. Early work [3] suggested a linear relationship but for high speed vehicles it has been shown [4 , 5] that a relationship of the form shown in Figure 2-3 is more appropriate since longer wavelengths are important. The modulus of the frequency response of the vehicle is related to the sine wave amplitude using a frequency response function, i.e.,

$$\begin{aligned} \left|U(if)\right| &= A\left|H(if)\right| \\ &= \alpha\sqrt{\lambda}\left|H(if)\right| \quad \ldots\ldots\ldots\ldots (2\text{-}43) \end{aligned}$$

where $f = \Omega/2\pi$ (Hz.), Ω being the circular frequency used earlier. Recognizing that the wave length is related to the

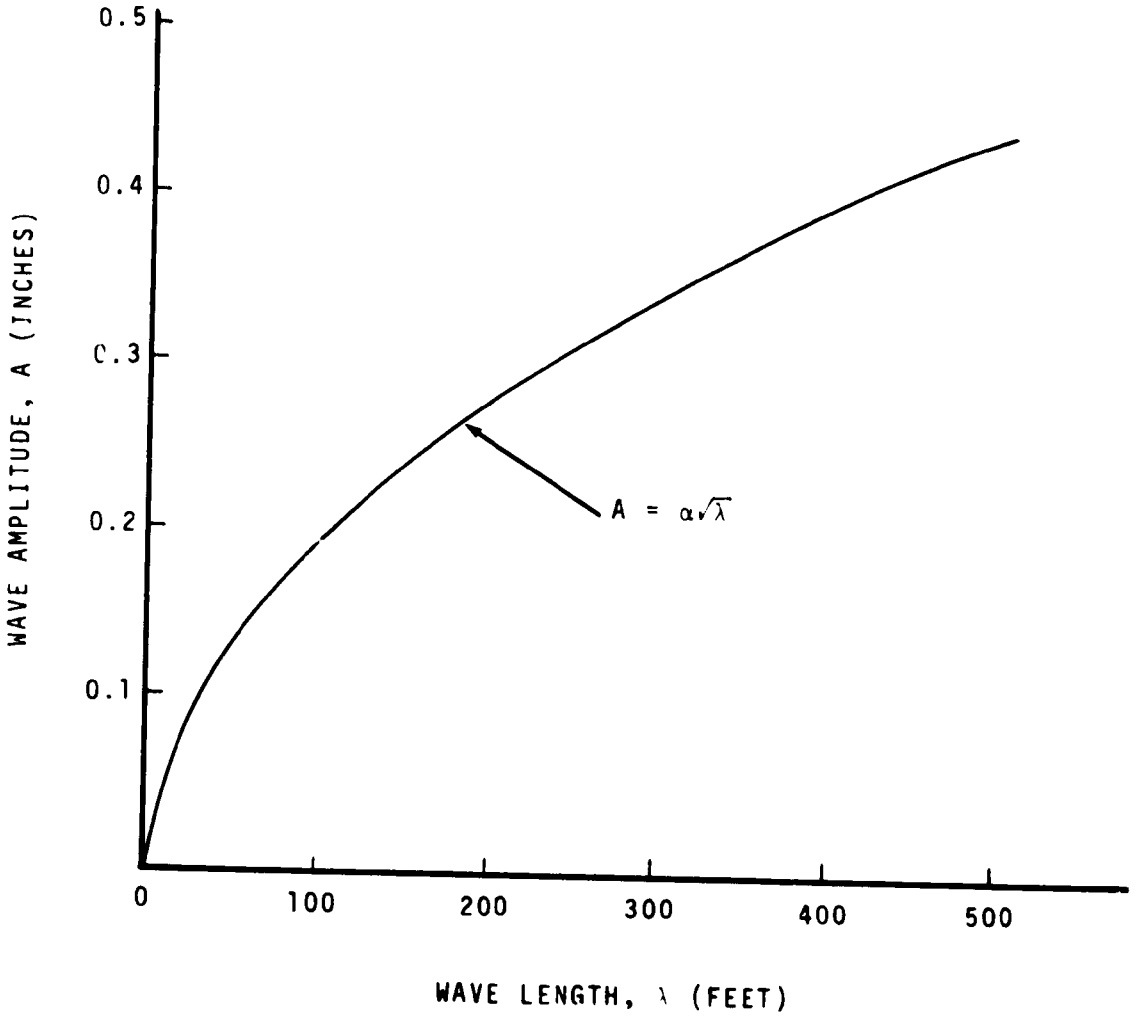

Figure 2-3 Representative Amplitude versus Wave Length Relationship

vehicle mean forward velocity, V, and sinusoidal irregularity frequency, f, one may alternatively write

$$\left| U(if) \right| = \frac{\alpha\sqrt{V}\,\left|H(if)\right|}{\sqrt{f}} \quad \ldots\ldots\ldots (2\text{-}44)$$

DYNALIST II calculates and plots the modulus of the frequency response function relating rail irregularity and coordinate location. This function is scaled by $\alpha\sqrt{V/f}$ to obtain sinusoidal response amplitude. Values for α are often given for particular rail system environments. It is a direct measure of rail roughness.

2.7 Random Rail Excitation

The theory of probabilistic structural dynamics has advanced in recent years to the state where it is now common to model rail irregularities as a stationary random process. A power spectral density function of rail irregularity is used to describe the magnitude of irregularity at various frequencies. A stationary random process assumes that the rail irregularity is invarient under a shift in spacial location and that the power spectral density is only a function of the correlation between irregularities at various spacial separations.

Rail irregularities are characterized using a spacial power spectral density function and this function tends to be of the analytical form

$$E(F) = K F^{-n} \quad \ldots\ldots\ldots (2\text{-}45)$$

In most cases it has been found that n is approximately equal to two. The parameter F is the frequency of irregularity in

cycles/foot, and K is a measure of roughness.

For a vehicle moving at a constant mean forward velocity, V, the corresponding temporal frequency due to irregularities is given by

$$f = V F \quad \text{cycles /sec} \quad . \quad . \quad . \quad . \quad . \quad . \quad . \quad . \quad (2\text{-}46)$$

and, therefore,

$$E(f) = KV^{n-1} f^{-n} \quad . \quad . \quad . \quad . \quad . \quad . \quad . \quad . \quad . \quad (2\text{-}47)$$

The response excited by this random rail irregularity may be either acceleration, velocity or displacement depending upon the form of the selected frequency response function. By definition, this function relates the input excitation, track irregularity, to the selected response output. If the frequency response function is denoted by the general form $H_u(if)$ then the variance of the response is

$$\text{Variance of Response} = \int_0^{+\infty} \left| H_u(if) \right|^2 E(f)\, df$$

$$= \int_0^{+\infty} S_u(f) df \quad . \quad . \quad . \quad . \quad . \quad . \quad (2\text{-}48)$$

where

$S_u(f)$ = power spectral density of response

The variance and power spectral density response at selected vehicle locations provide information to study many related problems. For example, the intensity of response maxima and zero crossing can be estimated from $S_u(f)$. Also, one can make estimates of the expected fatigue life of structural components as well as the probability associated with different response levels.

Section 2.5 showed that the rail irregularity at all wheel locations was related to a single rail irregularity function, see (2-38). Therefore, it is sufficient to define a single power spectral density function for the rail. The phase relationship discussed in Section 2.5 incorporates all of the other necessary input information.

3. VERIFICATION AND EXAMPLES

3.1 General

The DYNALIST II computer program based on the theoretical development of Chapter 2 was verified by independent computational means and used to execute a number of example problems. Both lateral and vertical rail vehicle models were considered. Stability analyses were made for the lateral models which include a six degree-of-freedom truck, a 14 d.o.f. car and a 42 d.o.f. three-car train. Three vehicle velocities were considered. In addition, response computations were made for the one-car and three-car lateral models. One-car and three-car vertical models were also generated and response computations were made for these configurations. Both sinusoidal and random response computations were made. The models and corresponding stability and response results are discussed in this chapter.

3.2 Test Problem: Lumped Mass Model

Frequency response computations using DYNALIST II for the four-degree of freedom lumped mass model shown in Figure 3-1 were verified using an alternate computer program. An independent solution was developed based on the Cramer's Rule approach. This approach recognized that the system frequency response function can be expressed in terms of the complex variable, s, as

$$\left([m]s^2 + [c]s + [k]\right)\left\{H_u(s)\right\} = \left\{A\right\} \qquad (3\text{-}1)$$

where $[m], [c], [k]$ = (4x4) system mass, damping and stiffness matrices.

$\left\{H_u(s)\right\}$ = (4x1) vector of transfer functions

$\left\{A\right\} = [0\ 0\ 0\ 1]^T$

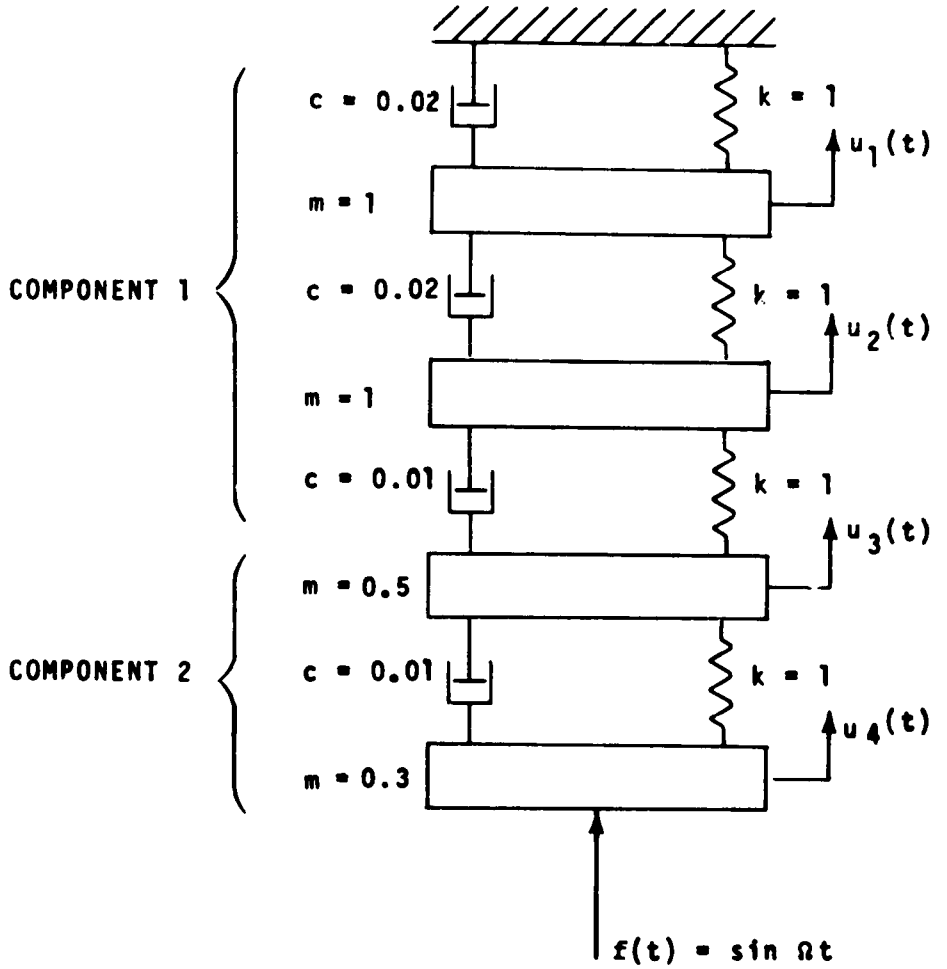

Figure 3-1. Four Degree of Freedom Test Problem

The solution to (3-1) for any element $H_{u_j}(s)$ of the vector $H_u(s)$ follows from the use of Cramer's rule wherein one obtains a ratio of determinates, i.e.,

$$H_{u_j}(s) = \frac{\det[N]}{\det[D]} \tag{3-2}$$

In this expression

$$[D] \equiv [m]s^2 + [c]s + [k]$$

and

$[N]$ = the matrix $[D]$ but with the jth column replaced by $\{A\}$.

Equation (3-2) may be written in the alternate form

$$H_{u_j}(s) = \frac{K\prod_{\ell}(s-\nu_\ell)}{\prod_{n}(s-\lambda_n)} \tag{3-2}$$

where

ν_ℓ = ℓth root of $[N]$, (a zero of the transfer function)

λ_n = nth root of $[D]$, (a pole of the transfer function)

K = root locus gain

A solution for the frequency response function ($H_{u_4}(i\Omega)$) was obtained by first evaluating the zeros, the poles and the root locus gain, and then letting $s = i\Omega$ over a range of frequencies.

The same problem was solved using DYNALIST II wherein the four-mass system was separated into two components. The first two masses and first three sets of spring/dashpot pairs comprised the first component and the remaining two masses comprised the

second. Complex modes were computed for the first component and both conjugate pairs were used to generate a complex component mode transformation. No modes were computed for the second component. A constraint equation was supplied to couple the system together and the resulting homogeneous equations were solved for the complex system eigenvalues and eigenvectors. These, in turn, were used to compute frequency response by modal summation. All of the modes were used. The results from DYANLIST II compared exactly with those generated by the Cramer's Rule method to within machine accuracy. The modulus of $H_{u_4}(i\Omega)$ is plotted in Figure 3.2. Preparation of input data for this example problem is discussed in Appendix C.

3.3 Lateral Models

Figure 2-2 shows the lateral model used for a single truck. Six degrees of freedom are noted and Table 3-1 gives the pertinent parameters of the truck.

A rigid car body model was used to study single car response. Figure 3-3(a) shows a schematic of the 14 degree-of-freedom car denoting 14 physical coordinates. Each truck has 6 coordinates. The car body coordinates are located at the geometric center of the body and include both displacement and rotation. The properties of the two trucks are indentical and are the same as those discussed in the previous paragraph, see Table 3-1. The car body was assigned a mass of 1,700 slugs and a rotational inertia of 1.85×10^6 slug-ft^2.

Figure 3-3(b) shows a schematic of the three car system used in this chapter. Each car is identical to the car discussed in the preceding paragraph. Note that the cars are attached using an elastic spring. The three-car model used in the stability analyses (Section 3.5) also included yaw springs with a spring rate of 2.5×10^6 ft-lb/rad between the car bodies.

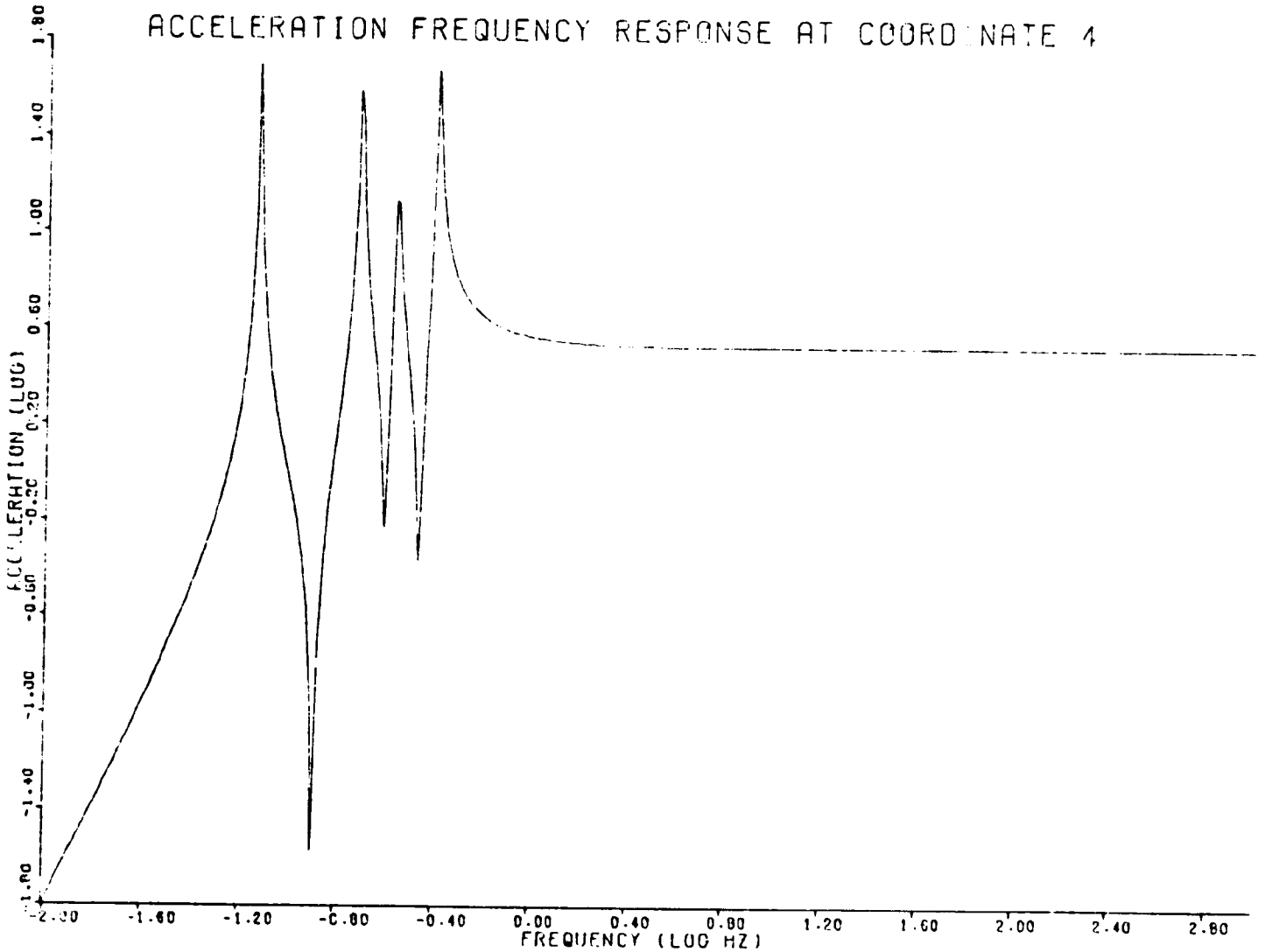

Figure 3-2 Frequency Response Function for the Lumped Mass Model

TABLE 3-1 PARAMETER VALUES FOR A SINGLE CAR
(LATERAL RESPONSE MODEL)

Description	Symbol	Value
Mass Properties		
Wheelset Mass	m_W	60 slugs
Wheelset Moment of Inertia	I_W	290 slug-ft^2
Truck Mass	m_T	250 slugs
Truck Moment of Inertia	I_T	2800 slug-ft^2
Car Body Mass	m_B	1700 slugs
Car Body Moment of Inertia	I_B	1.85×10^6 slug-ft^2
Primary Suspension		
Lateral Damping	C_1	0 lb sec/ft
Lateral Stiffness	K_1	5×10^5 lb/ft
Yaw Damping	C_2	0 ft lb sec/rad
Yaw Stiffness	K_2	3×10^7 lb/rad
Secondary Suspension		
Lateral Damping	C_3	1.55×10^3 lb sec/ft
Lateral Stiffness	K_3	1.75×10^4 lb/ft
Yaw Damping	C_4	0 ft lb sec/rad
Yaw Stiffness	K_4	5×10^6 ft lb/rad
Other Parameters		
Track Gage	$2L_o$	5 ft
Truck Wheelbase	L	8 ft
Mean Wheel Cone Angle	λ_o	.025 rad
Wheel Radius	r_o	1.33 ft
Creep Coefficient	F	3×10^6 lbs

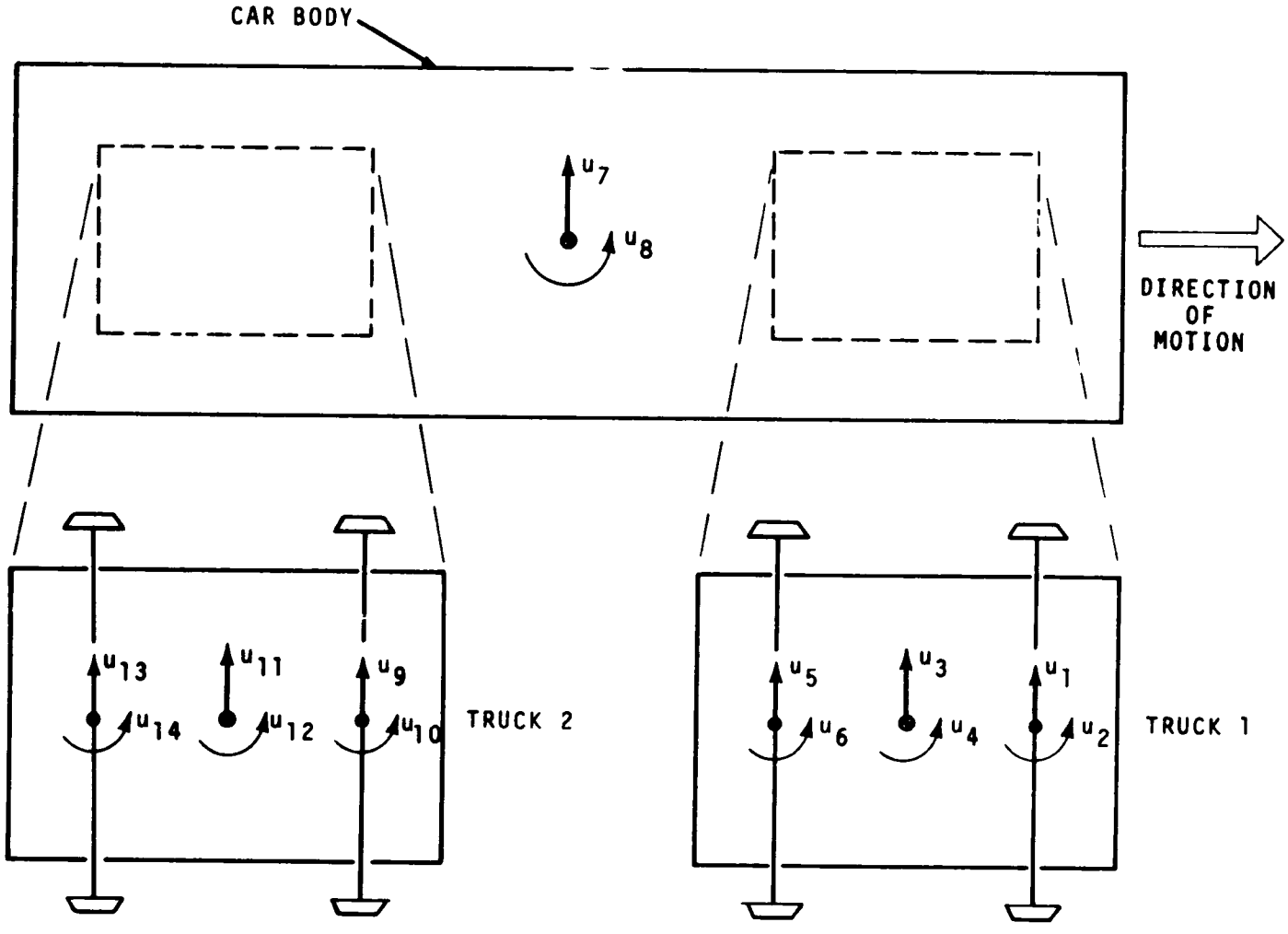

Figure 3-3(a). Plan View of Single Car Vehicle System (Lateral Response Model)

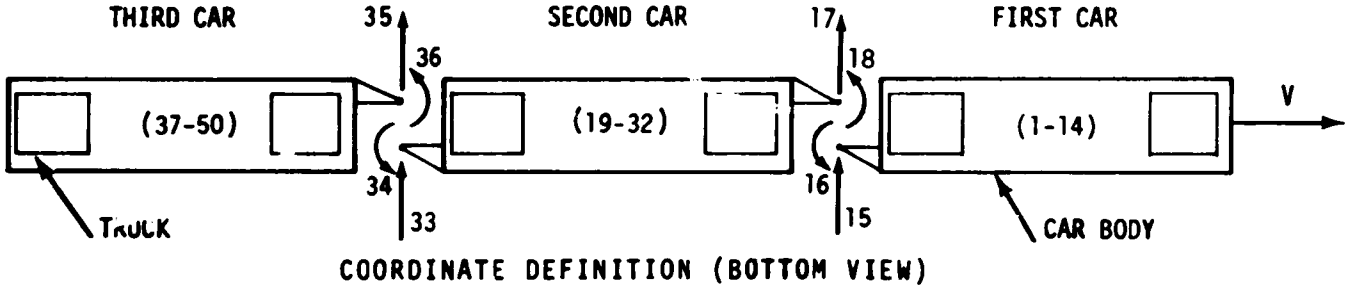

COORDINATE DEFINITION (BOTTOM VIEW)

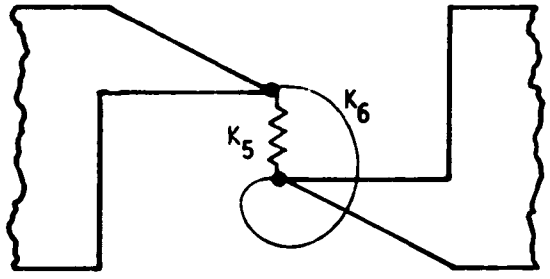

COUPLING DETAIL

Figure 3-3(b). Lateral Model of Three-Car Vehicle

3.4 Vertical Models

Vertical response studies were made for one and three-car vehicles. The single car model is shown in Figure 3-4. Spring stiffness elements are shown and it is noted that damping dashpots are located in the same positions and in parallel with the spring except for K_3. See Table 3-2 for parameter values.

It is noted that for the single car problem the system's mass, stiffness and damping matrices are entered in the p coordinate system; see Figure 3-4. These matrices are:

$$[m] = \text{mass matrix} = \begin{bmatrix} m_T & & & & & \\ & I_T & & & & \\ & & m_C & & & \\ & & & I_C & & \\ & & & & m_T & \\ & & & & & I_T \end{bmatrix}$$

$[k]$ = stiffness matrix =

$$\begin{bmatrix} (2K_1 + K_2) & 0 & -K_2 & -K_2\frac{L}{2} & 0 & 0 \\ 0 & \left(\frac{K_1 L_T^2}{2} + K_3\right) & 0 & -K_3 & 0 & 0 \\ -K_2 & 0 & 2K_2 & 0 & -K_2 & 0 \\ -K_2\frac{L}{2} & -K_3 & 0 & \left(\frac{K_2 L^2}{2} + 2K_3\right) & K_2\frac{L}{2} & -K_3 \\ 0 & 0 & -K_2 & K_2\frac{L}{2} & (2K_1 + K_2) & 0 \\ 0 & 0 & 0 & -K_3 & 0 & \left(\frac{K_1 L_T^2}{2} + K_3\right) \end{bmatrix}$$

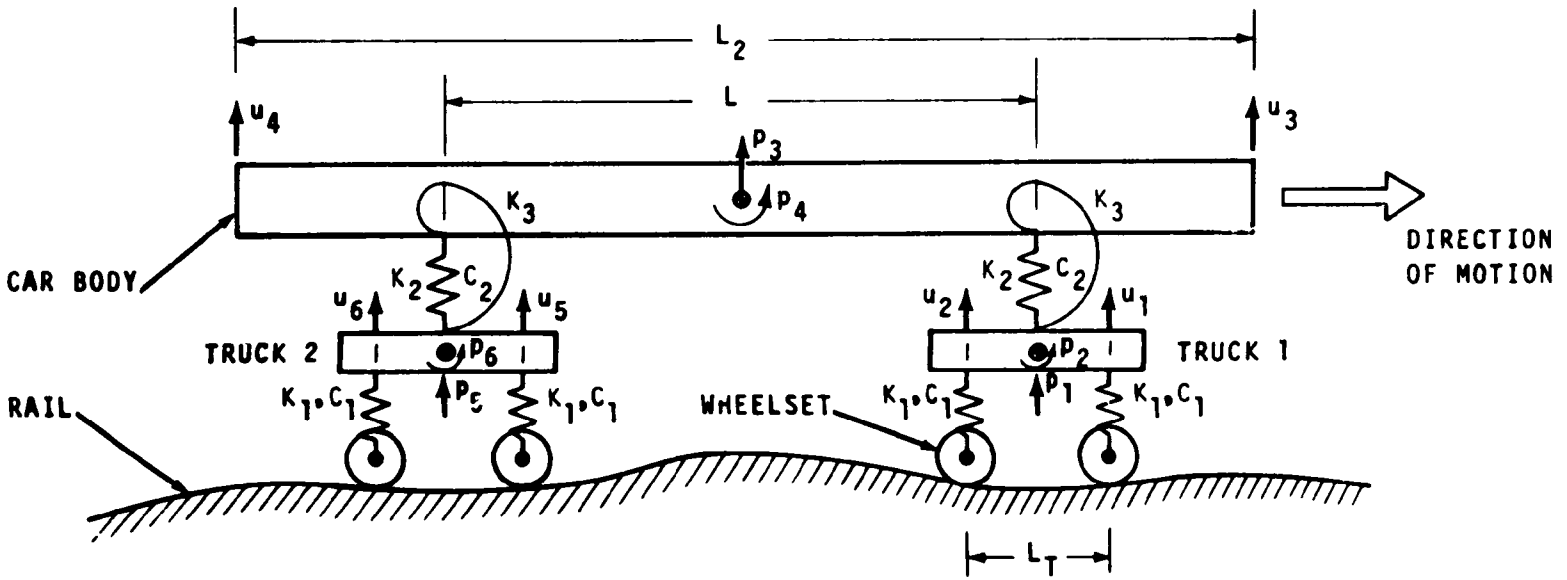

Figure 3-4 Elevation View of Vertical Single-Car Vehicle

TABLE 3-2 PARAMETER VALUES FOR A SINGLE CAR (VERTICAL RESPONSE MODEL)

Description	Symbol	Value
Mass Properties		
Truck Mass	m_T	250 slugs
Truck Moment of Inertia	I_T	2800 slug-ft^2
Car Body Mass	M_C	1700 slugs
Car Body Moment of Inertia	I_C	1.85×10^6 slug-ft^2
Primary Suspension		
Stiffness	K_1	3×10^5 lb/ft
Damping	C_1	2.1×10^4 lb-sec/ft
Secondary Suspension		
Stiffness	K_2	1.86×10^4 lb/ft
Damping	C_2	3.0×10^3 lb-sec/ft
Stiffness	K_3	4.5×10^5 ft-lb/rad
Other Parameters		
Truck Wheelbase	L_T	8 ft
Truck Centerline Separation	L	83 ft
Car Length	L_2	100 ft

$$[c] = \text{damping matrix} = \begin{bmatrix} 2C_1+C_2 & 0 & -C_2 & -C_2\frac{L}{2} & 0 & 0 \\ 0 & C_1\frac{L_T^2}{2} & 0 & 0 & 0 & 0 \\ -C_2 & 0 & 2C_2 & 0 & -C_2 & 0 \\ -C_2\frac{L}{2} & 0 & 0 & C_2\frac{L^2}{2} & C_2\frac{L}{2} & 0 \\ 0 & 0 & -C_2 & C_2\frac{L}{2} & 2C_1+C_2 & 0 \\ 0 & 0 & 0 & 0 & 0 & C_1\frac{L_T^2}{2} \end{bmatrix}$$

In the p coordinate system the equations of motion are

$$[m]\ \ddot{p} + [c]\ \dot{p} + [k]\ p = [c]\dot{\delta} + [k]\delta \quad \ldots\ldots \quad (3\text{-}3)$$

where δ = vertical track irregularity.

Note that the u coordinates are related to the p coordinates, see Figure 3-4, through the transformation matrix

$$\begin{Bmatrix} u_1 \\ u_2 \\ u_3 \\ u_4 \\ u_5 \\ u_6 \end{Bmatrix} = \begin{bmatrix} 1 & (L_T/2) & 0 & 0 & 0 & 0 \\ 1 & (-L_T/2) & 0 & 0 & 0 & 0 \\ 0 & 0 & 1 & (L_2/2) & 0 & 0 \\ 0 & 0 & 1 & (-L_2/2) & 0 & 0 \\ 0 & 0 & 0 & 0 & 1 & L_T/2 \\ 0 & 0 & 0 & 0 & 1 & L_T/2 \end{bmatrix} = \begin{Bmatrix} p_1 \\ p_2 \\ p_3 \\ p_4 \\ p_5 \\ p_6 \end{Bmatrix}$$

Also, the rail irregularities are input to the computer program in the u coordinate system by the $f_u(i\Omega)$ vector as

$$\left\{F_u(i\Omega)\right\} = \left\{\begin{array}{ll} i\Omega C_1 & K_1 \\ i\Omega C_1 e^{i\Omega L_T/V} & K_1 e^{i\Omega L_T/V} \\ 0 & 0 \\ 0 & 0 \\ i\Omega C_1 e^{i\Omega L/V} & K_1 e^{i\Omega L/V} \\ i\Omega C_1 e^{i\Omega (L+L_T)/V} & K_1 e^{i\Omega (L+L_T)/V} \end{array}\right\} \Delta(i\Omega)$$

The three car train model is composed of three identical cars. Each car has the properties of the car shown in Figure 3-4 and are as given in Table 3-2. The interface between each two adjacent cars has a vertical spring and a rotational spring.

3.5 Stability Analysis

DYNALIST II may be used to perform stability analyses whereby the eigenvalues and eigenvectors of the system are computed but no response computations are made. Eigenvalues are of the complex form

$$\Lambda_j = \sigma_j + i\,\omega_j \quad \ldots\ldots\ldots\ldots\ldots\ldots \quad (3\text{-}4)$$

The homogenous equations of motion therefore have solutions

$$y_j(t) = y_{o_j} e^{\Lambda_j t} = y_{o_j} e^{(\sigma_j \pm i\omega_j)t} \quad \ldots\ldots\ldots \quad (3\text{-}5)$$

where ω_j may be interpreted as a damped natural frequency and σ_j as a growth rate. The system is considered to be stable if and only if $\sigma_j < 0$ for all j. In the case of oscillatory modes where $\omega_j \neq 0$, the undamped natural frequency, ω_{o_j}, and critical damping ratio, ζ_j, are related to σ_j and ω_j by

$$\omega_{o_j} = \sqrt{\sigma^2 + \omega^2} \quad \ldots\ldots\ldots\ldots\ldots\ldots \quad (3\text{-}6)$$

$$\zeta_j = \sigma_j/\omega_{o_j} \quad \ldots\ldots\ldots\ldots\ldots\ldots \quad (3\text{-}7)$$

Stability analyses were made for three lateral model configurations at three velocities. The models include the Lateral Truck Model, Figure 2-2; the Lateral Car Model, Figure 3-3; and the Three-Car Train Model, Figure 3-4. The three velocities were 300, 450, and 600 ft/sec. Eigenvalues computed for these cases are presented in Tables 3-3 to 3-5. It may be noted that the critical damping ratios of the truck hunting modes go from approximately $\zeta = .43$ at $V = 300$ ft/sec to $\zeta = .08$ at $V = 600$ ft/sec. Eigenvectors corresponding to the first hunting mode of the single car vehicle are presented in Table 3-6 for the three velocities.

3.6 Response Analysis

Response computations were made for both lateral and vertical vehicle models. Two models were considered in each case, a single car and a three-car model. Random type rail irregularities were input to the lateral models* and sinusoidal type

*Except for the three-car model for which only frequency response functions were computed.

TABLE 3-3 EIGENVALUES FOR LATERAL TRUCK MODEL

V = 300 ft/sec		V = 450 ft/sec		V = 600 ft/sec	
σ	ω	σ	ω	σ	ω
-2.163 E+2	2.362 E+2	-1.129 E+2	3.131 E+2	-8.580 E+1	3.320 E+2
-3.011 E+2	1.591 E+0	-1.441 E+2	2.858 E+2	-1.080 E+2	3.012 E+2
-1.589 E+2	2.476 E+2	-1.723 E+2	7.372 E+0	-1.056 E+2	2.526 E+1
-6.662 E+1	7.363 E+1	-5.238 E+2	6.868 E+1	-6.003 E+1	8.167 E+1
-1.828 E+1	6.701 E+1	-2.541 E+1	7.872 E+1	-2.357 E+1	8.699 E+1
-6.092 E+0	1.421 E+1	-5.513 E+0	2.238 E+1	-2.212 E+0	2.771 E+1 *

*Truck hunting mode

TABLE 3-4 EIGENVALUES FOR SINGLE CAR VEHICLE

V = 300 ft/sec		V = 450 ft/sec		V = 600 ft/sec		
σ	ω	σ	ω	σ	ω	
-2.163 E+2	2.362 E+2	-1.128 E+2	3.131 E+2	-8.580 E+1	3.320 E+2	
-2.163 E+2	2.362 E+2	-1.128 E+2	3.131 E+2	-8.580 E+1	3.320 E+2	
-3.011 E+2	1.591 E+0	-1.441 E+2	2.858 E+2	-1.080 E+2	3.012 E+2	
-3.011 E+2	1.591 E+0	-1.441 E+2	2.858 E+2	-1.080 E+2	3.012 E+2	
-1.589 E+2	2.476 E+2	-1.723 E+2	7.373 E+0	-1.056 E+2	2.525 E+1	
-1.589 E+2	2.476 E+2	-1.723 E+2	7.373 E+0	-1.056 E+2	2.525 E+1	
-6.662 E+1	7.363 E+1	-5.240 E+1	6.867 E+1	-6.005 E+1	8.168 E+1	
-6.661 E+1	7.362 E+1	-5.241 E+1	6.864 E+1	-6.005 E+1	8.167 E+1	
-1.834 E+1	6.696 E+1	-2.548 E+1	7.872 E+1	-2.361 E+1	8.698 E+1	
-1.838 E+1	6.692 E+1	-2.544 E+1	7.871 E+1	-2.359 E+1	8.697 E+1	
-6.074 E+0	1.419 E+1	-5.480 E+0	2.232 E+1	-2.198 E+0	2.764 E+1	*
-6.210 E+0	1.412 E+1	-5.592 E+0	2.223 E+1	-2.300 E+0	2.755 E+1	*
-1.256 E+0	5.912 E+0	-1.298 E+0	5.918 E+0	-1.316 E+0	5.918 E+0	
-8.468 E-1	4.408 E+0	-8.535 E-1	4.405 E+0	-8.562 E-1	4.404 E+0	

*Truck hunting modes

TABLE 3-5 EIGENVALUES FOR LATERAL THREE-CAR MODEL

V = 300 ft/sec		V = 600 ft/sec		
σ	ω	σ	ω	
8.730 E-2	2.854 E+2	-4.738 E-1	2.852 E+2	
-2.649 E-1	2.338 E+2	-6.488 E-1	2.336 E+2	
-6.040 E+0	1.423 E+1	-2.195 E+0	2.770 E+1	*
-6.074 E+0	1.419 E+1	-2.195 E+0	2.769 E+1	
-6.212 E+0	1.412 E+1	-2.198 E+0	2.764 E+1	
-6.033 E+0	1.418 E+1	-2.192 E+0	2.764 E+1	
-6.187 E+0	1.411 E+1	-2.297 E+0	2.756 E+1	
-6.060 E+0	1.415 E+1	-2.301 E+0	2.755 E+1	
-1.255 E+0	6.061 E+0	-1.315 E+0	6.034 E+0	
-1.075 E+0	5.334 E+0	-1.108 E+0	5.328 E+0	
-9.038 E-1	4.648 E+0	-9.209 E-1	4.638 E+1	
-8.468 E-1	4.408 E+0	-8.562 E-1	4.404 E+0	

*Truck hunting modes

TABLE 3-6 TRUCK HUNTING MODE FOR SINGLE CAR VEHICLE

COORD.	V = 300 ft/sec		V = 450 ft/sec		V = 600 ft/sec	
	REAL	IMAG.	REAL	IMAG.	REAL	IMAG.
1	8.019 E-1	2.373 E-1	6.564 E-1	3.602 E-1	5.610 E-1	3.897 E-1
2	-2.433 E-2	3.103 E-2	-2.899 E-2	2.266 E-2	-3.043 E-2	1.879 E-2
3	8.217 E-1	1.135 E-1	7.614 E-1	2.887 E-1	7.441 E-1	3.296 E-1
4	-1.790 E-2	3.102 E-2	-2.358 E-2	2.387 E-2	-2.585 E-2	2.052 E-2
5	7.901 E-1	-4.792 E-2	7.140 E-1	1.151 E-1	6.542 E-1	1.712 E-1
6	-2.405 E-2	3.377 E-2	-2.939 E-2	2.504 E-2	-3.120 E-2	2.091 E-2
7	-1.051 E-1	-4.804 E-2	-3.719 E-2	-6.507 E-2	-1.453 E-2	-6.155 E-2
8	2.690 E-4	-1.428 E-3	6.992 E-4	-3.816 E-4	7.104 E-4	-6.140 E-5
9	1.000 E+0	0.000	9.127 E-1	1.284 E-1	8.258 E-1	1.599 E-1
10	-1.722 E-2	4.369 E-2	-2.333 E-2	3.874 E-2	-2.479 E-2	3.638 E-2
11	9.783 E-1	-1.464 E-1	1.000 E+0	0.000	1.000 E+0	0.000
12	-9.849 E-3	4.151 E-2	0.000	3.779 E-2	-1.877 E-2	3.605 E-2
13	8.892 E-1	-3.215 E-1	8.710 E-1	-1.784 E-1	8.210 E-1	-1.325 E-1
14	-1.597 E-2	4.673 E-2	-2.276 E-2	4.165 E-2	-2.458 E-2	3.915 E-2

rail irregularities were input to the vertical models. Results of these computations are discussed in this section.

The input power spectral density function describing lateral rail irregularities is shown in Figure 3-5. The sloping portion of the function is given by

$$E(f) = KVf^{-2} \quad \ldots\ldots\ldots\ldots\ldots\ldots \quad (3\text{-}8)$$

where $K = 1.85 \times 10^{-7}$ ft^2 and V = 450 ft/sec. The low frequency (long wavelength) portion of the spectrum has been limited somewhat arbitrarily to reflect the tendency of waviness to be limited at longer wavelengths.

In computing the lateral response of the single car vehicle, all of the modes were retained, i.e., the solution is "exact". Acceleration response functions for three points on the vehicle are plotted in Figures 3-6(a,b) through 3-8(a,b). Subfigure (a) of each pair corresponds to frequency response while subfigure (b) corresponds to power spectral density of response. Units of acceleration are in ft/sec^2. Response points are identified in Table 3-7 which lists RMS acceleration response in g's.

TABLE 3-7 ACCELERATION RESPONSE FOR LATERAL SINGLE CAR MODEL

Figure No.	Coordinate No.	Response Point Identification	RMS Acceleration (g's)
3-6	11	Car body sway at attachment point of trailing truck	.0248
3-7	15	Truck sway at center of mass of trailing truck frame	.1590
3-8	17	Wheelset sway at center of mass of trailing wheelset, trailing truck.	.1290

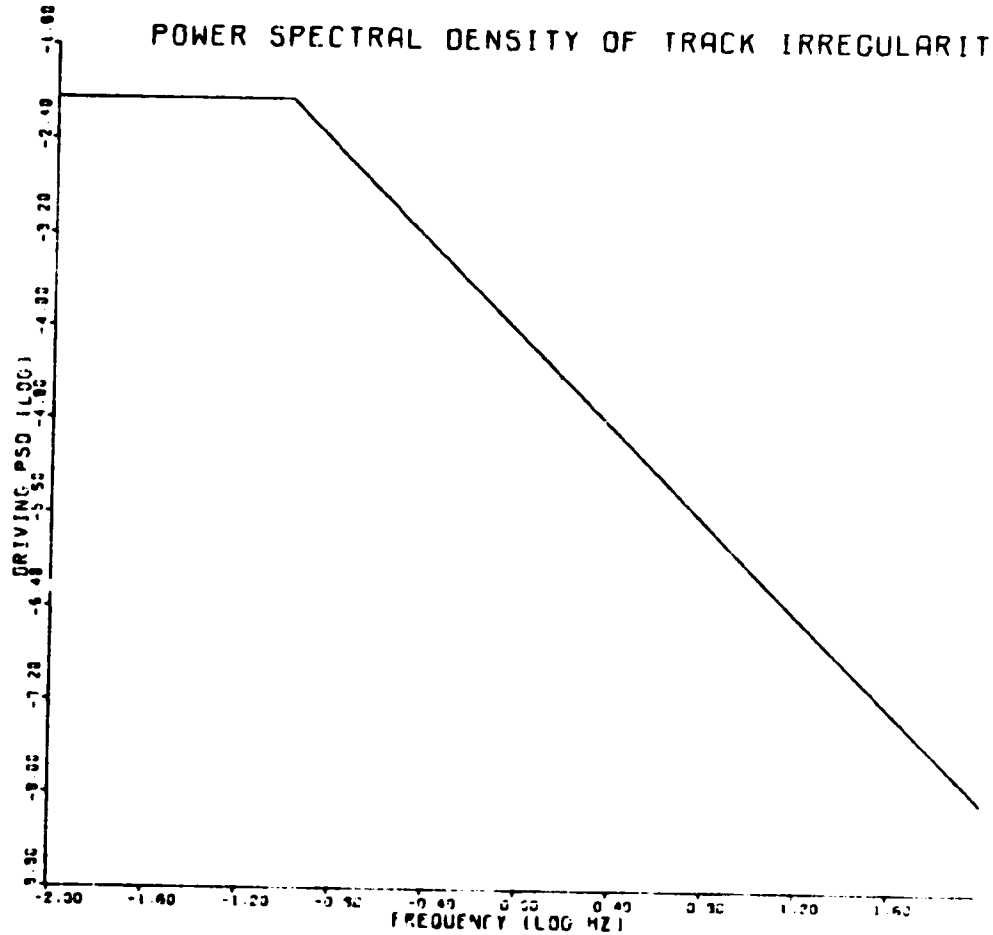

Figure 3-5. Power Spectral Density of Lateral Track Irregularity for V=450 ft/sec.

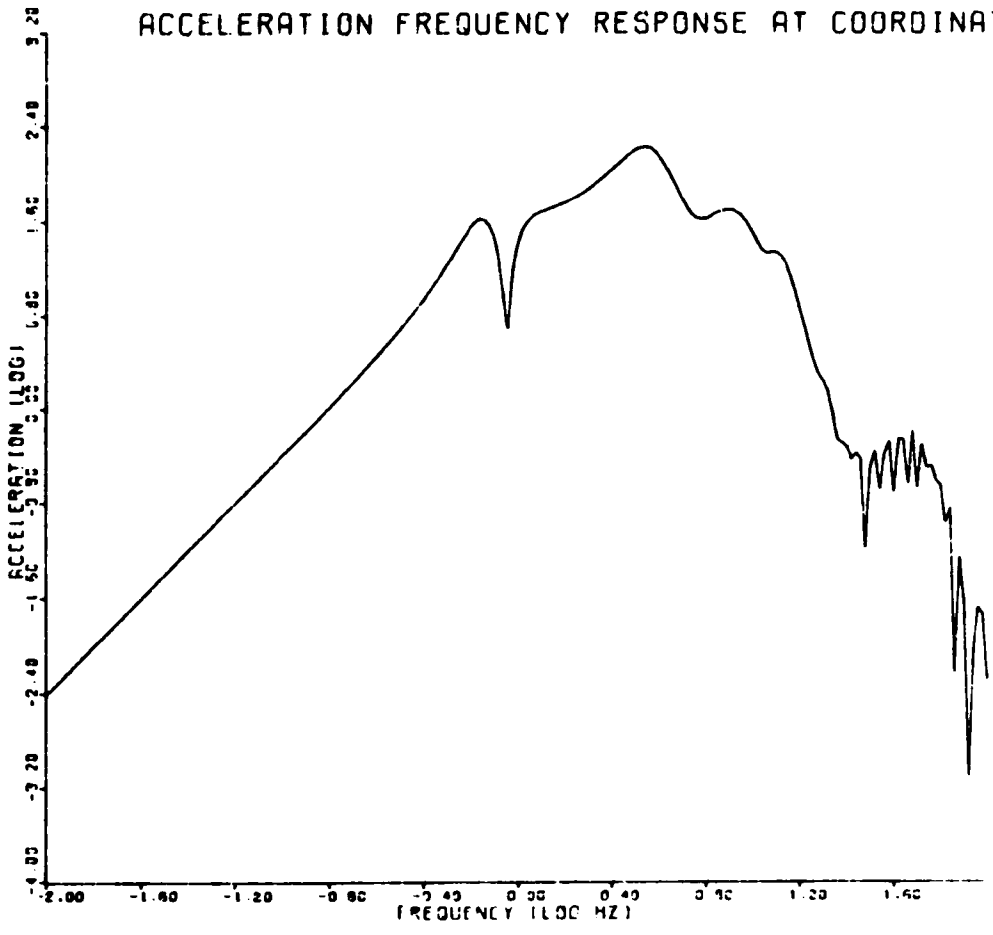

Figure 3-6(a). Acceleration Frequency Response, Single Car Lateral Model, Car-Body Sway

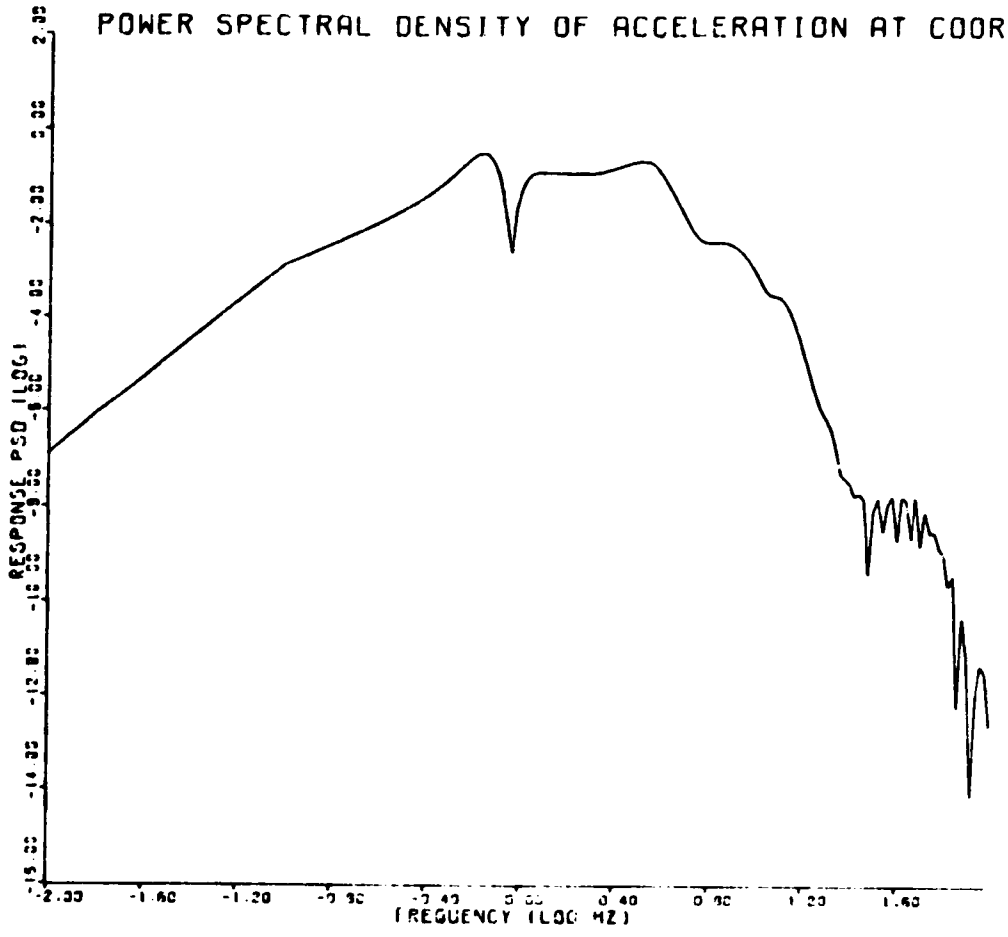

Figure 3-6(b). Acceleration PSD, Single Car Lateral Model, Car-Body Sway

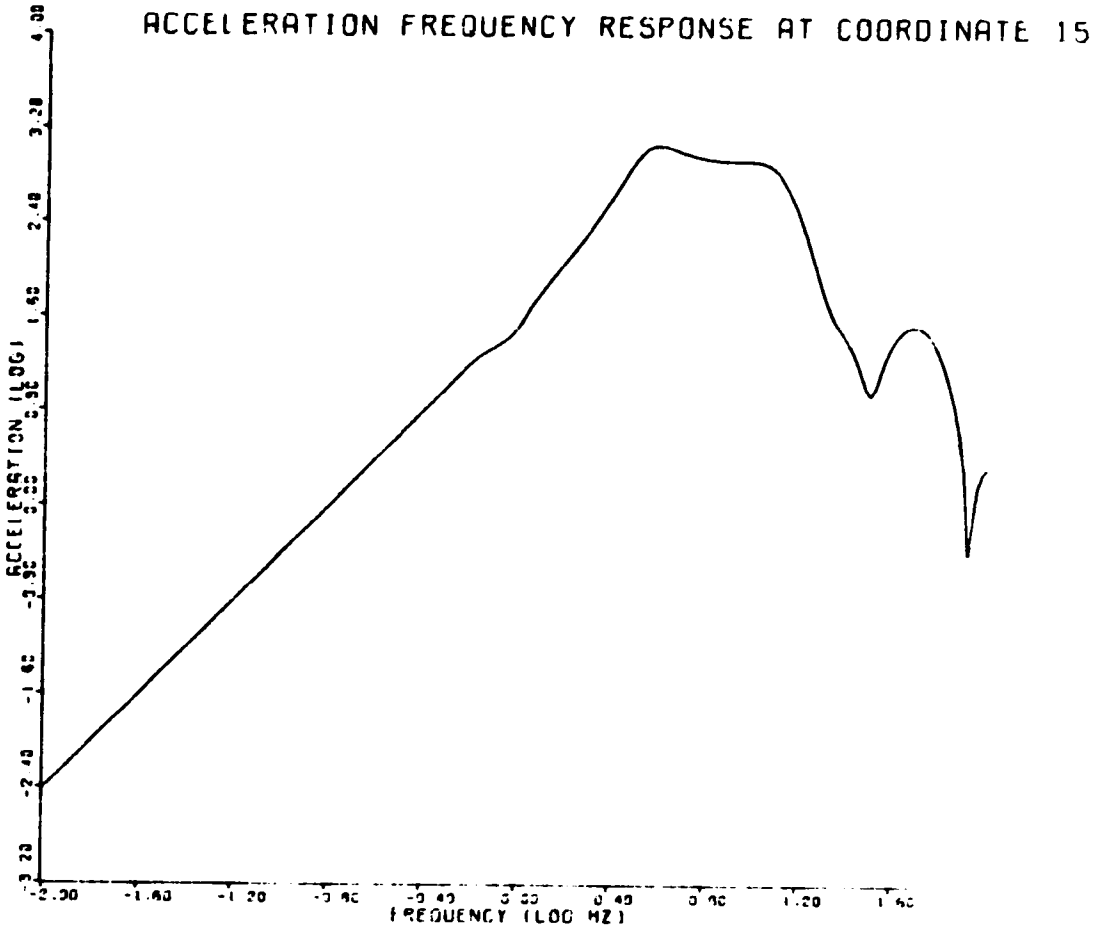

Figure 3-7(a). Acceleration Frequency Response, Single Car Lateral Model, Truck Sway

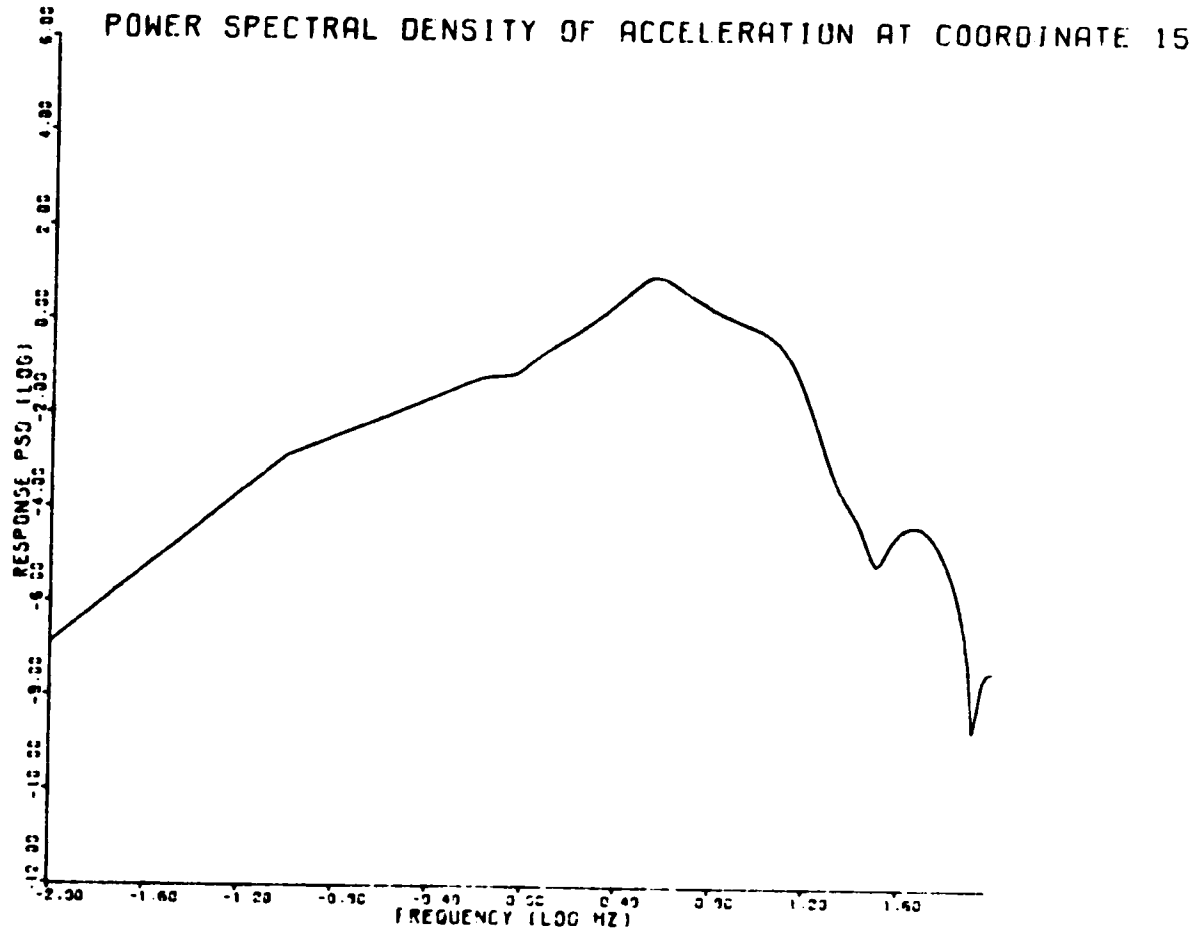

Figure 3-7(b). Acceleration PSD, Single Car Lateral Model, Truck Sway

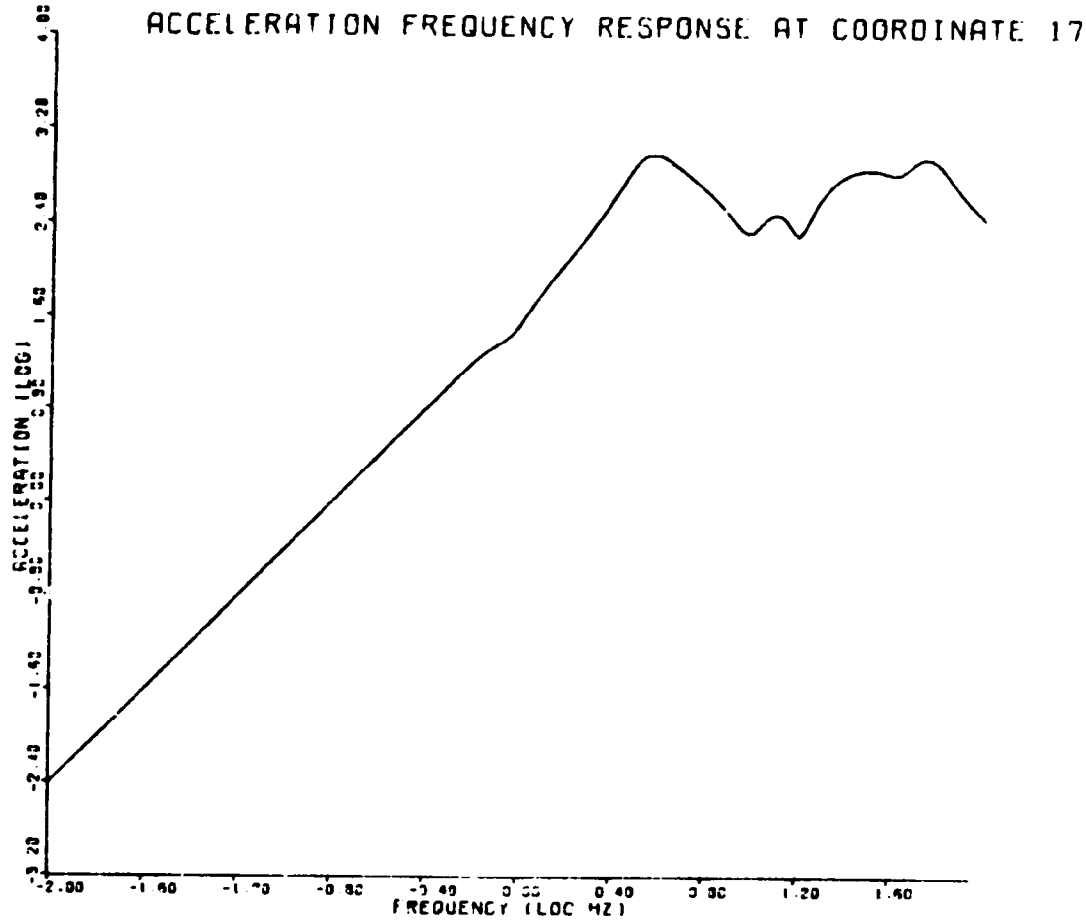

Figure 3-8(a). Acceleration Frequency Response, Single Car Lateral Model, Wheelset Sway

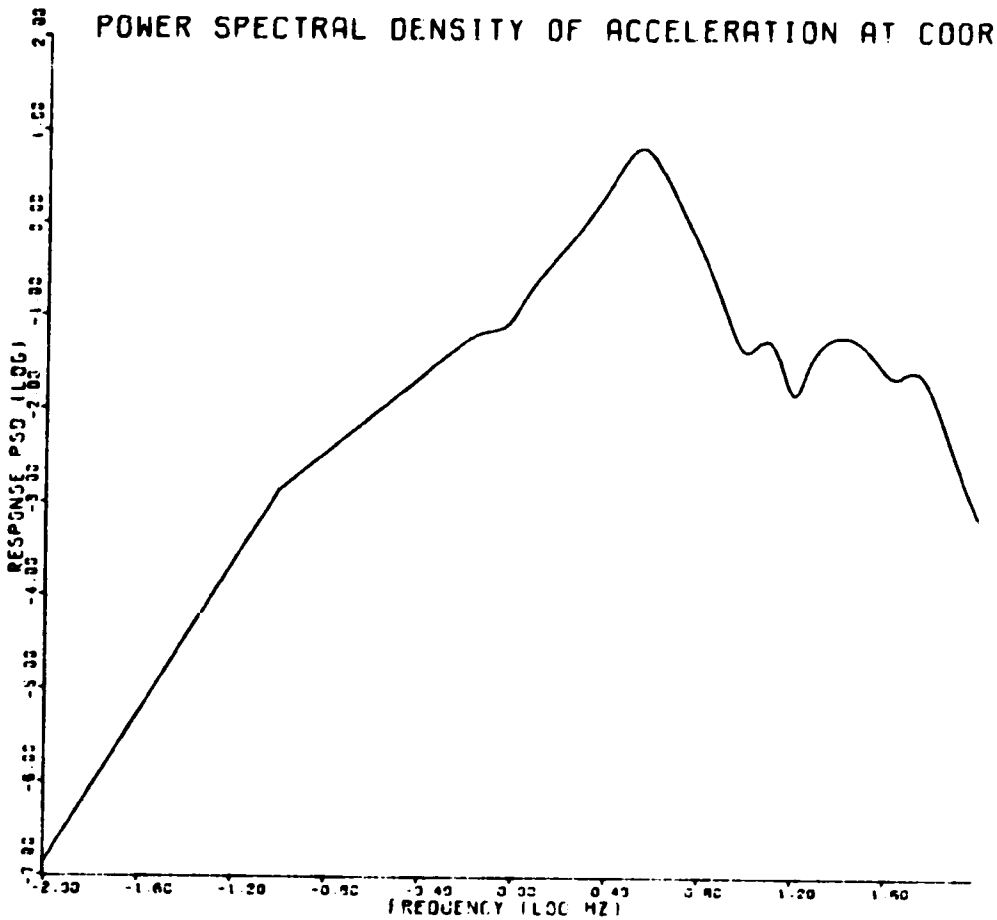

Figure 3-8(b). Acceleration PSD, Single Car Lateral Model, Wheelset Sway

Lateral acceleration frequency response at three points on the three-car train was computed by modal synthesis where six conjugate pairs of modes were retained for each car. Frequency response plots are shown in Figures 3-9 through 3-11. Response points are identified in Table 3-8.

TABLE 3-8 ACCELERATION RESPONSE FOR LATERAL THREE-CAR MODEL

Figure No.	Coordinate No.	Response Point Identification
3-9	15	Car body sway of leading car at coupling point with middle car
3-10	33	Car body sway of middle car at coupling point with trailing car
3-11	43	Car body sway at center of mass of trailing car

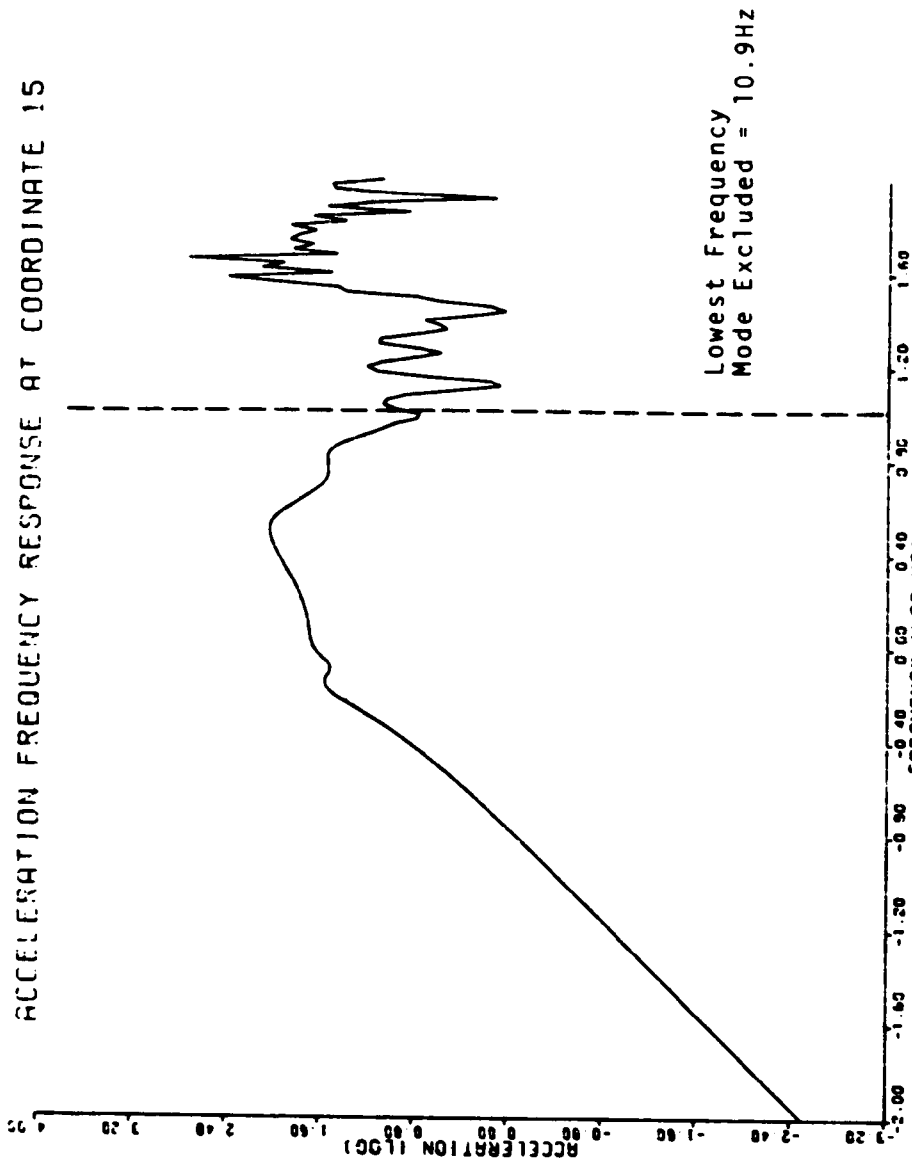

Figure 3-9. Acceleration Frequency Response, Three Car Lateral Model, Leading Car Sway

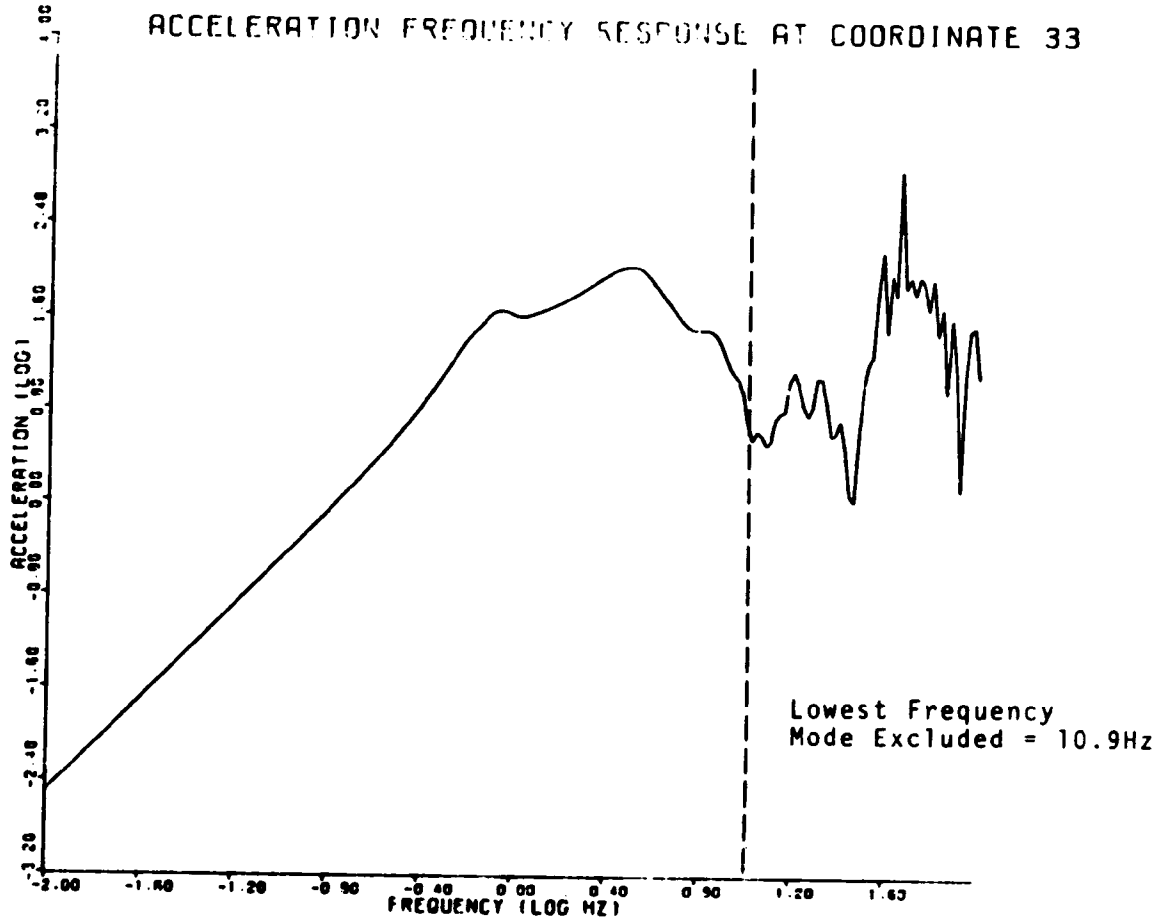

Figure 3-10. Acceleration Frequency Response, Three Car Lateral Model, Middle Car Sway

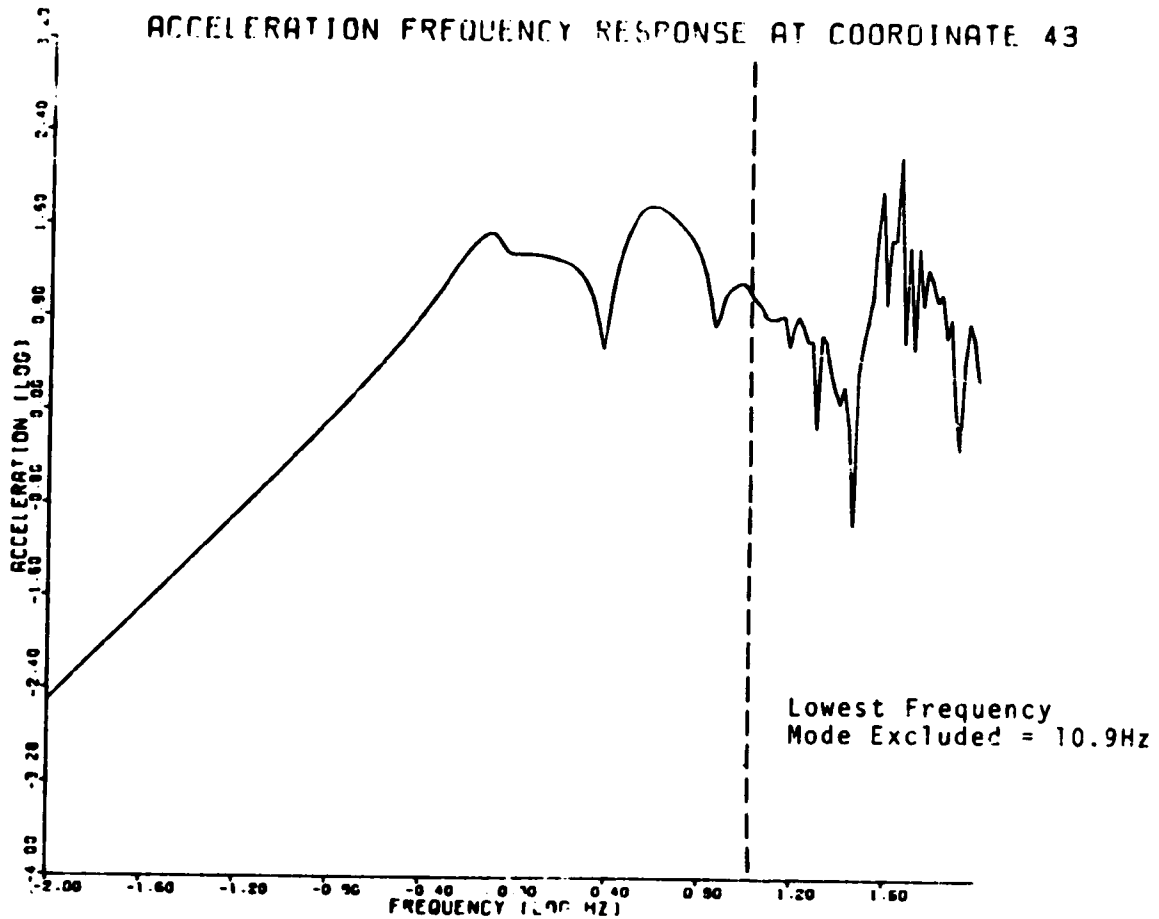

Figure 3-11. Acceleration Frequency Response, Three Car Lateral Model, Trailing Car Sway

Vertical response studies were made using sinusoidal rail irregularities of amplitude $A = \alpha\sqrt{\lambda}$ where $\alpha = 4.52 \times 10^{-3}$. This roughness parameter corresponds to an amplitude of 0.5 inches at a wavelength of 85 ft. Amplitude A is plotted as a function of frequency f in Figure 3-12.

A special option in the program was developed for computing response directly for a system without recource to the subsystems approach. This option was used in an attempt to compute vertical response for the single car vertical model. However, the results appeared to be incorrect and are therefore not presented. It must be concluded at the present time that a computational bug still exists in the code implementing this option and users are cautioned to avoid its use.

Vertical acceleration response was evaluated for the three-car vertical model, however, and these results appear to be correct. In generating this model, very stiff vertical springs, $K = 7.5 \times 10^7$ lb/ft, were used to couple adjacent ends of car bodies in the train. The intent here was to try to represent a hinged connection. Consequently, two lightly damped high frequency car body modes were computed, (37.1 and 45.4 Hz.). The existance of these modes appears to cause a severe vibrational environment in this frequency range. Although such an environment is unrealistic for real trains, it appears to be reasonable for the specified model and results are therefore included. Frequency response and corresponding sinusoidal response plots are shown in Figures 3-13(a,b) through 3-15 (a,b). Table 3-9 lists the peak acceleration in g's experienced over the frequency range below 25 Hz. (log 25 = 1.40), for several locations on the vehicle. Response points are identified therein. Computations were made using all of the component modes; only four modes for each component occurred in complex conjugate pairs. The rest were real.

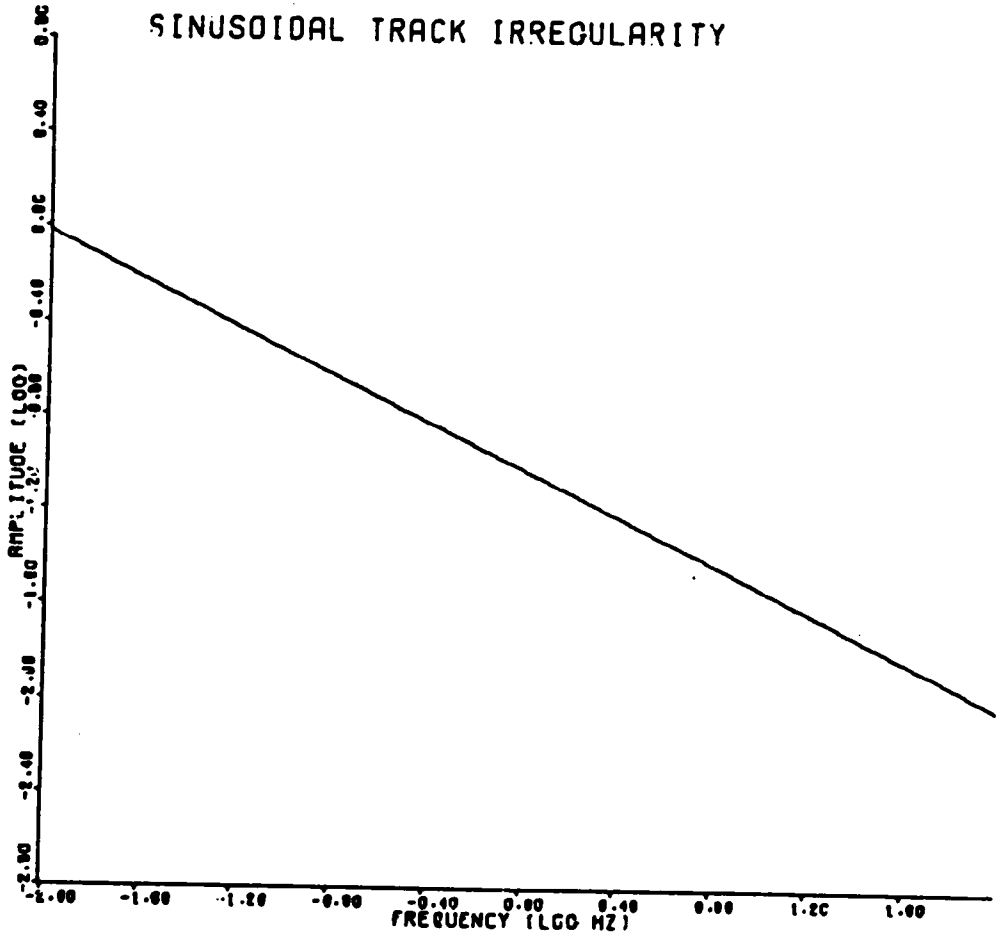

Figure 3-12. Amplitude of Sinusoidal Track Irregularity versus Frequency

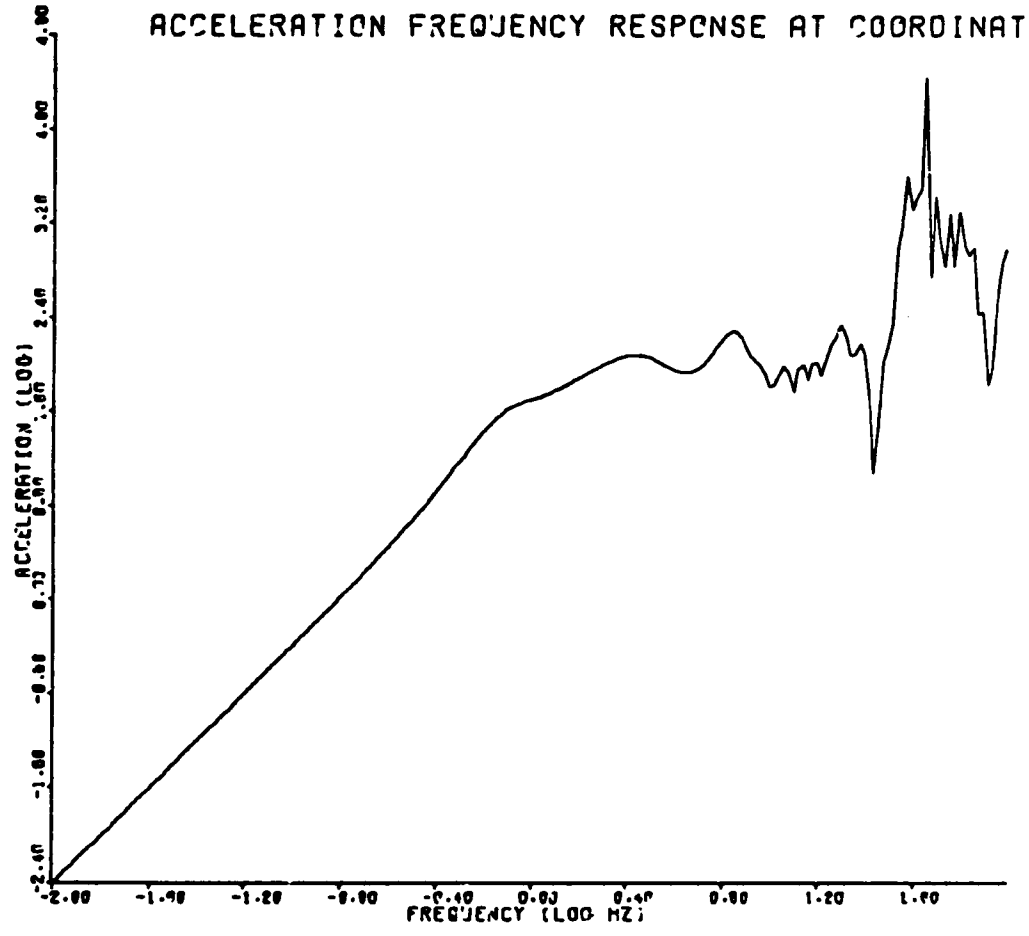

Figure 3-13(a). Acceleration Frequency Response, Three Car Vertical Model, Middle Car Leave.

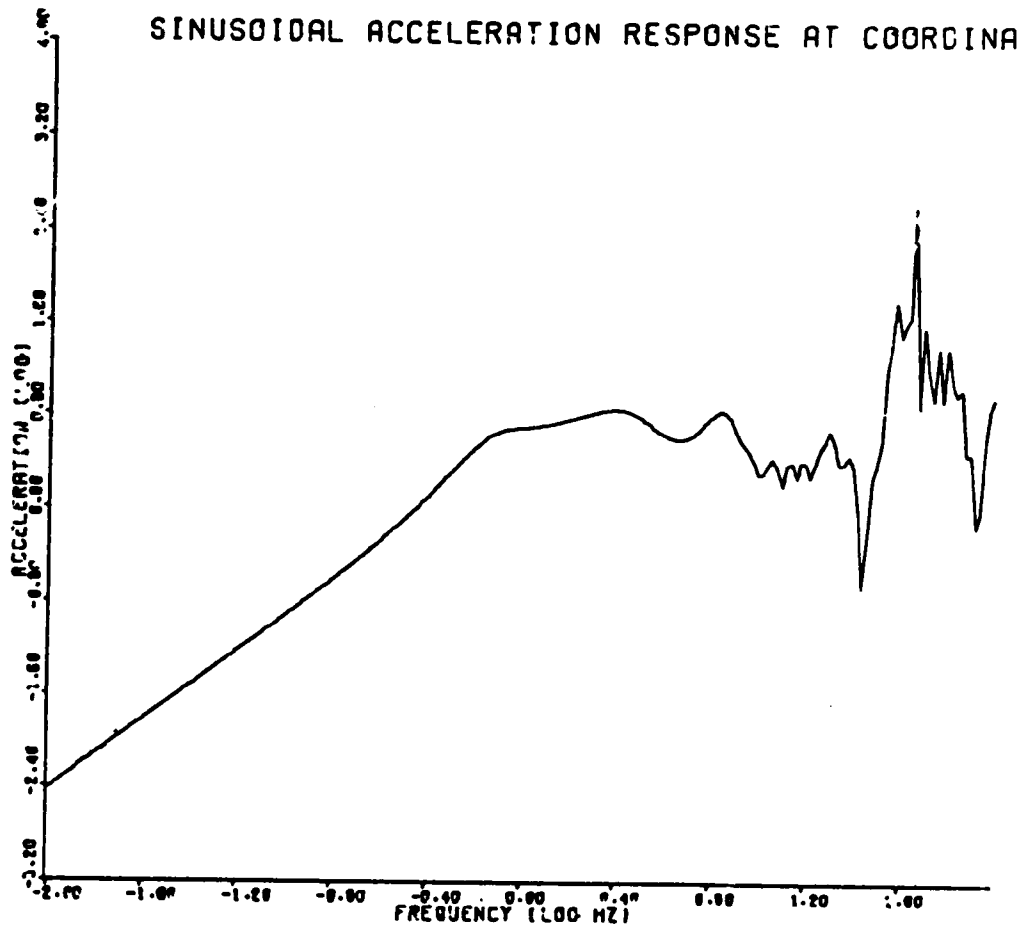

Figure 3-13(b). Sinusoidal Acceleration Response, Three Car Vertical Model, Middle Car Heave.

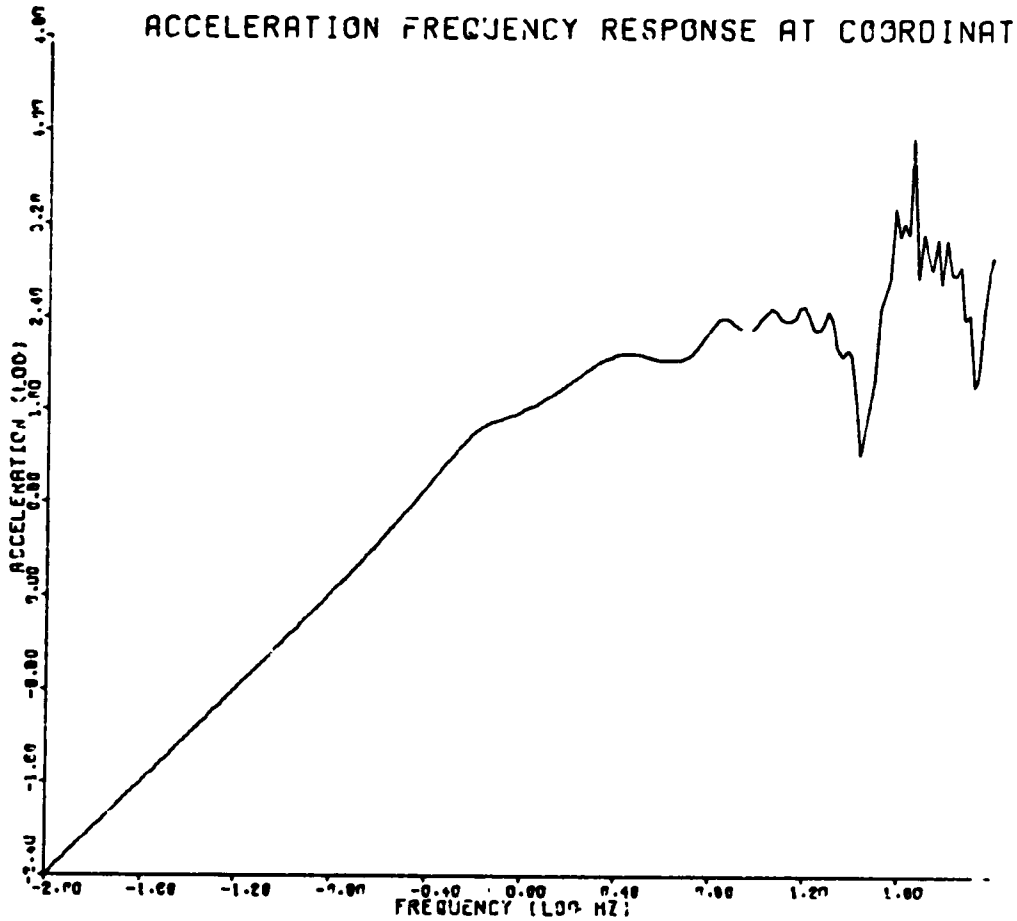

Figure 3-14(a). Acceleration Frequency Response, Three Car Vertical Model, Trailing Car Heave.

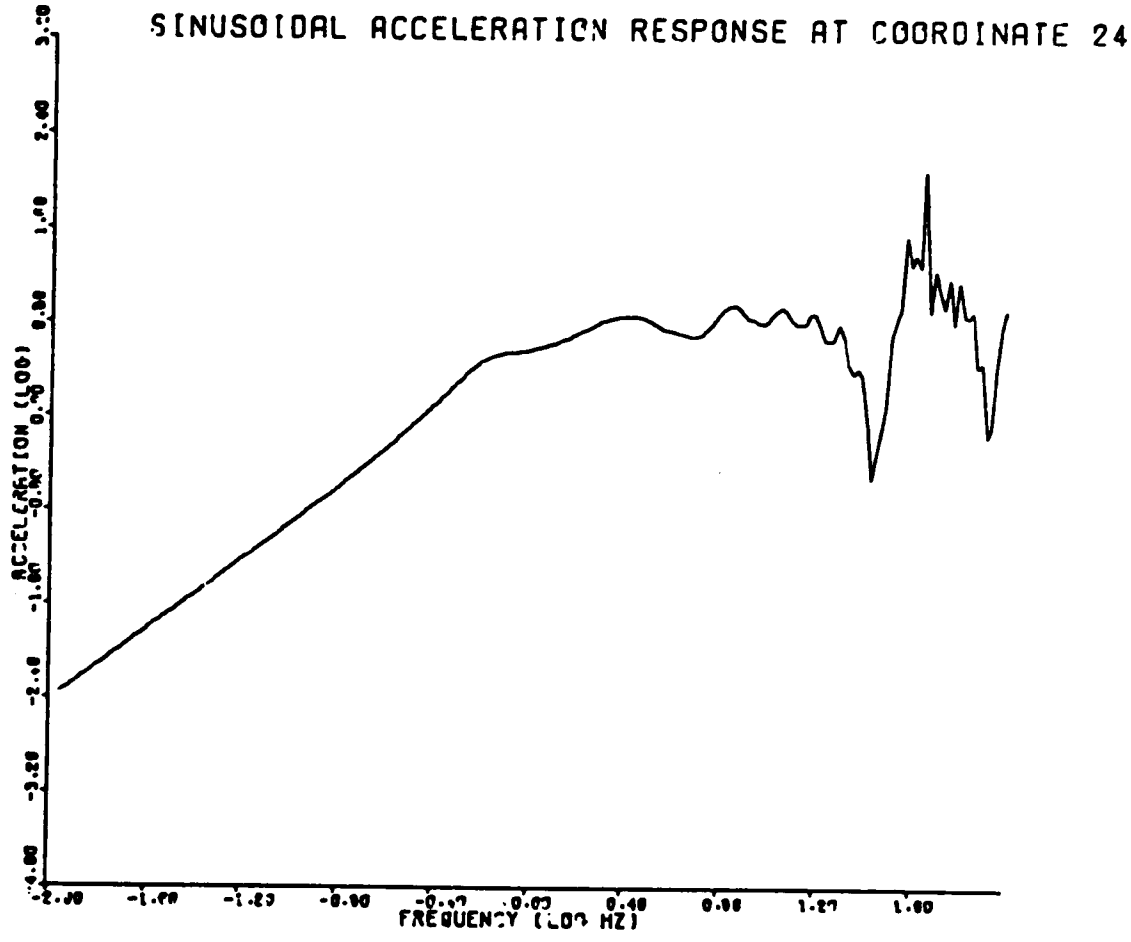

Figure 3-14(b). Sinusoidal Acceleration Response, Three Car Vertical Model, Trailing Car Heave.

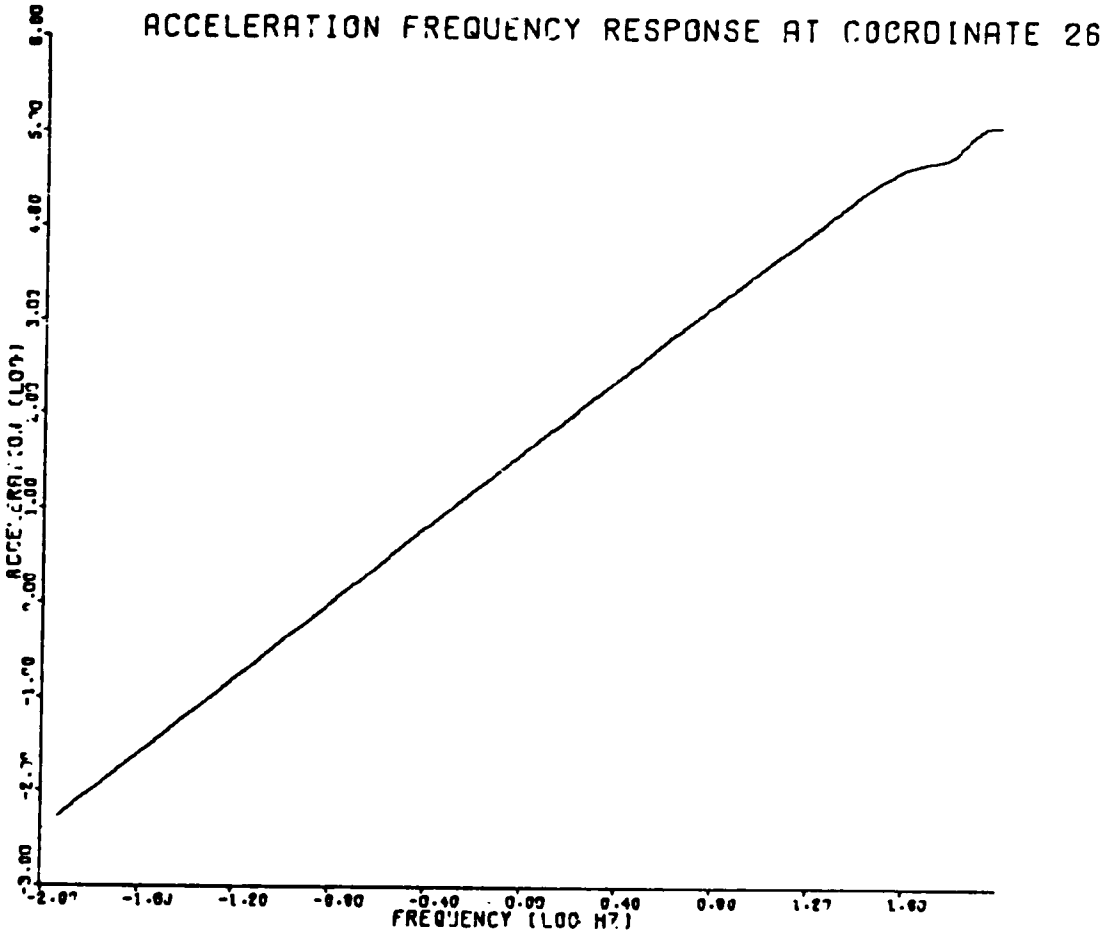

Figure 3-15(a). Acceleration Frequency Response, Three Car Vertical Model, Trailing Truck Heave, Trailing Car.

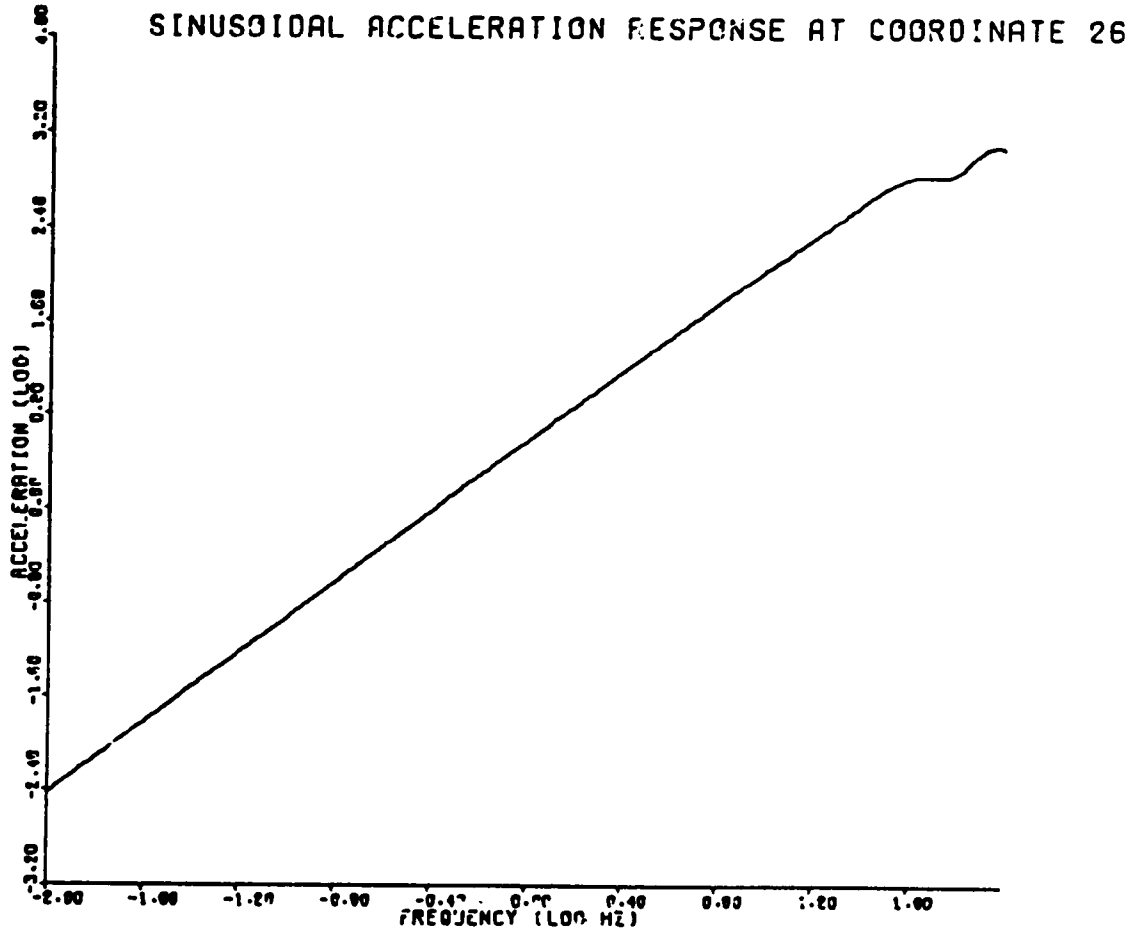

Figure 3-15(b). Sinusoidal Acceleration Response, Three Car Vertical Model, Truck Heave, Trailing Car.

TABLE 3-9 ACCELERATION RESPONSE FOR THE VERTICAL THREE-CAR MODEL

Figure No.	Coordinate No.	Response Point Identification	Peak Accl. (g's)
3-13	14	Car body heave, middle car at attachment point to trailing car.	.222
3-14	24	Car body heave, trailing car, trailing end.	.280
3-15	26	Truck heave, trailing car, trailing end of truck.	12.60

A very high acceleration level for the truck is noted. In fact, the frequency response curve is observed to follow the line $|H(i\Omega)| = \Omega^2$ over almost all of this range. This merely indicates that the primary suspension is so stiff that the truck frame essentialy follows the rail irregularity.

3.7 Convergence

In Figures 3-9 through 3-11, the high frequency response characteristics appear to be in error. The vertical dotted lines show the lowest frequency of the excluded component modes. Certainly, one would not expect the approximate response solutions to be valid beyond this point. In fact, one may even question whether the solution is good near the frequency of the highest included mode. Experience with various modal synthesis procedures applied to classical structural systems indicates that the accuracy of eigenvalues and eigenvectors deteriorates somewhere in the frequency range between 50% and 80% of the range spanned by the included modes [6]. This depends greatly on the system, of course, as well as the procedure being used. As more and more modes are included in the synthesis, eigenvalues and eigenvectors as well as frequency response tend to become more accurate. The approximate solutions tend to converge to the "exact" ones, so called because they include all of the modes, and therefore no truncation error.

Three distinct problems in convergence have been identified with regard to the present application. The first one is the usual one associated with eigenvalue and eigenvector accuracy. While no particular study of this problem has yet been made, some feel for the problem can be gained from the results presented in [1, 2, 7]. Further insight in the classical mode case is provided by [8].

The other two problems concern the convergence of frequency response. One may anticipate at least one of these problems from the strange high frequency behavior exhibited in Figures 3-9 to 3-11 where acceleration frequency response has been plotted. Figures 3-16 (*a*, b, c) show plots of displacement frequency

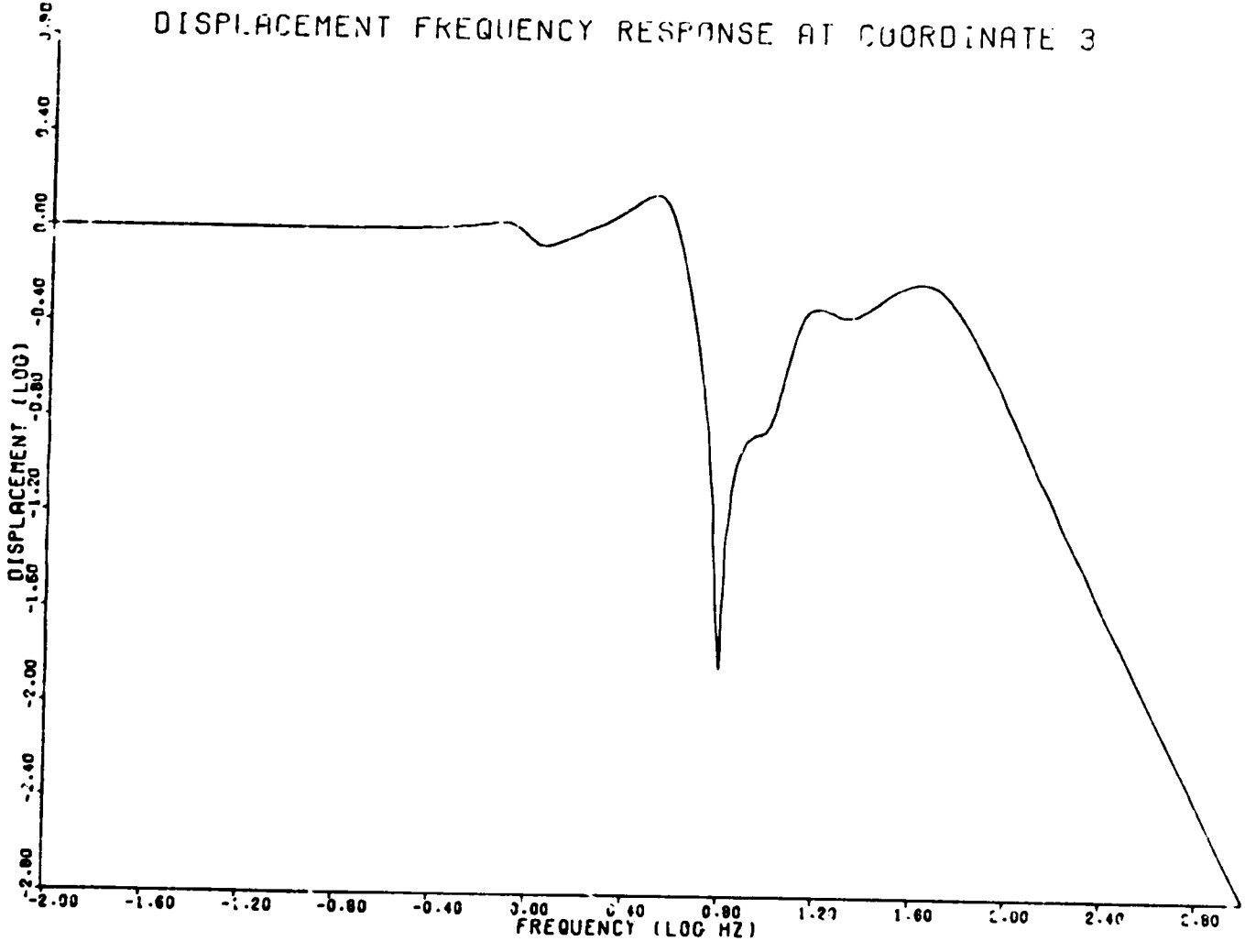

Figure 3-16(a). Displacement Frequency Response, Single Car Lateral Model, Leading Truck Center of Mass Sway - All Modes Retained.

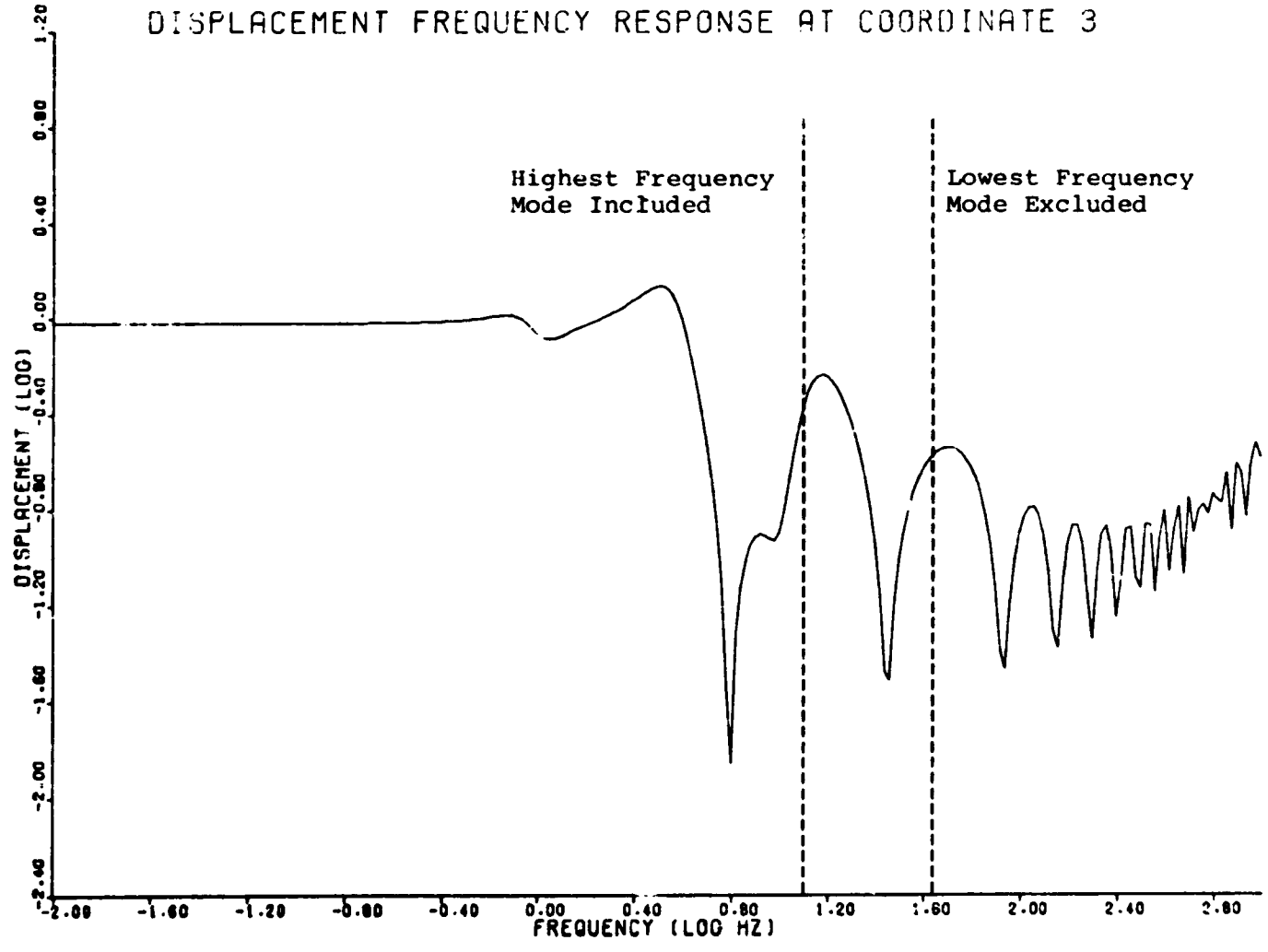

Figure 3-16(b). Displacement Frequency Response, Single Car Lateral Model, Leading Truck Center of Mass Sway - Four Conjugate Pairs of Modes Retained.

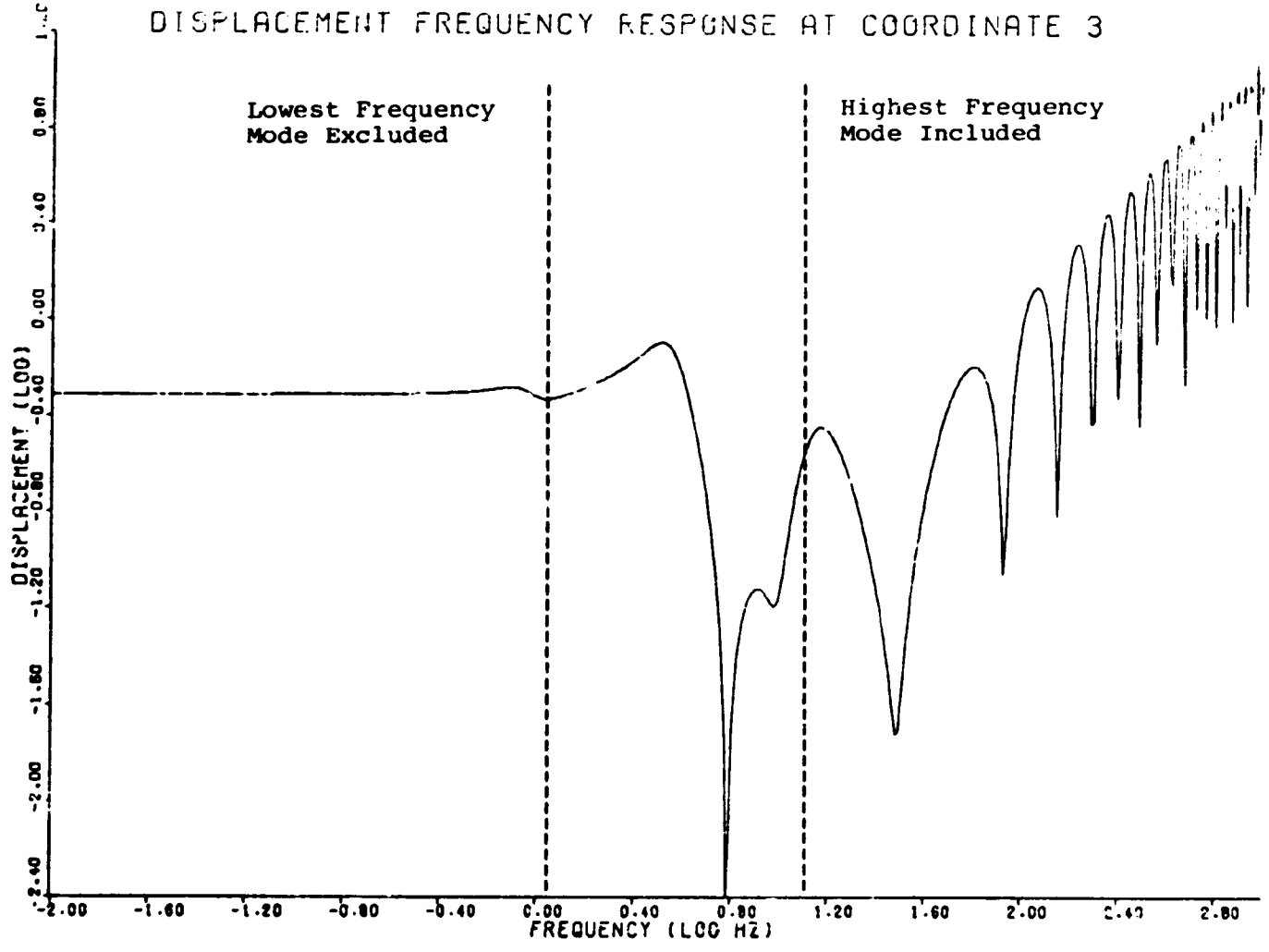

Figure 3-16(c). Displacement Frequency Response, Single Car Lateral Model, Leading Truck Center of Mass Sway - Three Conjugate Pairs of Modes Retained.

response for the leading truck frame center of mass on the lateral car model.* Figure 3-16(a) shows the "exact" solution obtained by including all of the modes. Figures 3-16(b) and 3-16(c) show frequency response computed for the same coordinate but with truncated mode solutions. Each truck was modeled as a component of the system. Figure 3-16(b) represents a solution where four out of six conjugate pairs of truck modes were included for each truck and Figure 3-16(c) represents a solution where only three out of the six were included. Both of these truncated mode solutions show significant error in the high frequency range. In both cases, the highest frequency mode included was 12.53 Hz (corresponding to ω = 78.72 and log (12.53) = 1.10). In Figure 3-16(b) the lowest frequency mode excluded was 45.49 Hz (ω = 285.8 and log (45.49) = 1.66). In Figure 3-16(c) the lowest frequency mode excluded was 1.17 Hz (ω = 7.373 and log (1.17) = .0695). From Table 3-4 (V = 450 ft/sec) one observes that (b) corresponds to inclusion of the lowest four pairs of eigenvalues (ranked by modulus) while (c) corresponds to inclusion of the lowest three pairs. Although the fourth pair has a very low frequency, it is almost critically damped. Thus, the modulus of its eigenvalue is larger than that of the mode with a frequency of 12.53 Hz.

The high frequency portion of the response spectrum is not the only place of interest. One of the most striking differences among the three plots is in the low frequency region where the frequency response function levels off. In moving from Figure 3.16(a) to Figure 3.16(c), one may observe that the "static" response (also called the Bode Gain) drops progressively lower than the correct value of unity. This result was somewhat surprising at first, since the appearance of Equation (2-41) seems to suggest that the contribution of higher order modes to the total frequency response diminishes with the reciprocal of the

*In this case, the wheelset yaw equations corresponded to (A-18) of Appendix A instead of (A-19). This accounts for the notch which occurs at a frequency of 6.2 Hz. and is probably responsible for the way the high frequency response takes off in the truncated mode solutions. The $\ddot{\delta}$ term in (A-18) has negligible effect in the low frequency range.

eigenvalues Λ. Further consideration reveals, however, that the "static" response is quite independent of the eigenvalues and should be obtained by other means.

For example, one may consider a simple two-degree-of-freedom spring mass system which is base excited by a sinusoidal displacement function $\delta(t)$. Two classical modes may be derived for this system. If one attempts to predict the low frequency response of the system by considering only one of the two modes, his solution will clearly be in error unless the eigenvector associated with the first mode exhibits the same displacement for both masses. Otherwise, the two masses will displace by different amounts and one knows on physical grounds that both masses will tend to move with the base as the excitation frequency approaches zero.

The solution of this problem is straightforward. One may evaluate the low frequency response of the system based upon a direct solution of the equations where the acceleration and velocity terms are neglected. The low frequency modal solution may be subtracted from this leaving a residual. This residual response represents the low frequency contribution by all of the unused modes. It may be added to the frequency response functions as a constant over the entire frequency range of interest. Such a procedure was proposed in [9,10], for example.

Formally, one may recall Equation (2-25). Transformation to the frequency domain results in

$$(K - \Omega^2 M + i \Omega C) H_q (i \Omega) = \bar{F}_q (i \Omega) \ldots (3\text{-}9)$$

where

$$\bar{F}_q (i \Omega) = \bar{\beta}^T \phi^T \bar{F}_u (i \Omega) \ldots\ldots (3\text{-}10)$$

and $\bar{F}_u$ (i Ω) is of the form given by (2-37). Neglecting terms in (3-9) which contain Ω, one obtains

$$K H_{q_o} = \bar{F}_{q_o} = \bar{\beta}^T \phi^T \bar{F}_{u_o} \quad \ldots\ldots\ldots \quad (3-11)$$

Solution of (3-11) leads to

$$H_{u_o} = \phi \bar{\beta} K^{-1} \bar{\beta}^T \phi^T \bar{F}_{u_o} \quad \ldots\ldots\ldots \quad (3-12)$$

The residual contribution of the unused modes to the response at low frequencies is then

$$H_{u_R} = H_{u_o} - H_u \text{ (i } \Omega) \big|_{\Omega \to o} \quad \ldots\ldots \quad (3-13)$$

where H_u (i Ω) is given by (2-42). Adding this residual term to H_u (i Ω) should result in an approximatation, $\hat{H}_u$ (i Ω), to the "exact" frequency response function which is accurate at all frequencies below some cut-off point which <u>then</u> would depend on eigenvalue separation, i.e.,

$$\hat{H}_u \text{ (i } \Omega) = H_u \text{ (i } \Omega) + H_{u_R} \quad \ldots\ldots \quad (3-14)$$

The modification suggested by (3-14) is not included in the present version of DYNALIST II. In cases where elements of the vector H_{u_o} are known to be unity, it is relatively easy to compensate for the residual error in one's interpretation of results. However, for some models this will not be the case. An example is the lateral truck model shown in Figure 2-2 which is "tied to ground" through lateral and yaw springs. In this case, low frequency displacements will not be unity. In situations such as this, it is recommended that modal truncation be used only with appropriate caution.

In general, further study is required in order to take proper advantage of the modal truncation option. In any application it must first be determined whether the desired system eigenvalues and eigenvectors have been obtained to within an acceptable degree of accuracy. Then, assuming that the low frequency

problem is corrected, an upper limit on the range of accurate frequency response must be established. As one additional step, it must be determined whether the RMS response integrated over this range has converged to an upper limit if this measure of response is to be used in the case of random rail irregularities.

4. CONCLUSIONS AND RECOMMENDATIONS

The original DYNALIST computer program for dynamic analysis of rail vehicle systems has been modified and extended in the new version, DYNALIST II. In addition to computing the complex system eigenvalues and eigenvectors for stability analyses, DYNALIST II offers the capability for computation of vehicle response to either sinusoidal or random track irregularities.

4.1 Conclusions

As a result of this development effort, a number of conclusions may be drawn. These conclusions are briefly summarized in the paragraphs which follow.

Two major modifications have been made in the original part of the program. The first modification was to change the input coordinate space from u to p to facilitate the modeling of flexible structural elements and/or components. Whereas the user previously had to enter component equations of motion in the physical discrete coordinate space u, he may now enter component equations of motion in modal form and use the ϕ transformation to revert back to the physical coordinates for interpretation of output. This represents a significant improvement in that very complicated structural elements can now be included in the model without having to input complete finite element mass and stiffness matrices. Only portions of the real eigenvectors associated with response points, attachment points and forcing function inputs need be included in ϕ.

The other modification has resulted in automating the generation of the coordinate reordering vector IARANG. The user need

only specify which of the redundant coordinates are to be eliminated by the constraint equations. In the past, the need to input this vector did pose some problems for the inexperienced user.

In formulating the response capability, a special kind of frequency response function was defined. Normally, frequency response is interpreted as a characteristic of the system between two specified points on the system. In the case of rail vehicles, track inputs occur everywhere the system contacts the guideway so that frequency response associated with any particular contact point is not particularly meaningful. Since the inputs at each contact point are phased due to different parts of the vehicle traversing the same irregularities at different times, the force "distribution" is not of the classical form. However, the distribution is independent of guideway parameters so that a meaningful frequency response function between a scalar function defining guideway irregularity and any point on the system can be defined. This function is computed in the response portion of the program and can be plotted as well as printed.

Frequency response functions representing normalized response at selected vehicle locations are used in evaluating both sine and random response. Sine response is computed from a track roughness parameter. The variation of sine amplitude with wavelength is predetermined. Random response is computed from an input power spectral density describing the distribution of amplitude with frequency. The power spectral density of vehicle response may be plotted as well as printed, and the function is integrated over a specified frequency range to determine RMS response.

A number of example problems were developed to demonstrate the program. Both vertical and lateral models are included. Vehicles consisting of a single train car and several cars coupled together have been modeled. Stability and response analyses were made. Results of these analyses have been summarized.

As with any new computer program intended for general usage, some problems were encountered in running the examples. The two main problems are of a general nature and users should be aware of them so that they may be avoided. Both of the problems are numerical and are problem dependent. The first problem involves the occurrence of repeated roots, i.e. identical or nearly identical eigenvalues. When components of the system are identical and virtually isolated from each other by very weak coupling, numerical problems may occur in the eigenvalue/eigenvector subroutines. The problems encountered to date have been circumvented by perturbing system parameters by a small amount, say less than one percent, so that repeated roots do not occur.

The other problem has to do with the convergence of approximate solutions resulting from modal truncation. Three separate problems related to convergence were described in Section 3.7. The problems may be overcome by appropriate selection of component modes. At the present time, no foolproof guidelines can be provided. The user must either avoid modal truncation, or through his experience with a particular problem, make his own judgment as to which modes to select. This subject is beyond the scope of the present effort but is certainly deserving of further research.

4.2 Recommendations

Based on experience gained with DYNALIST II to date, the following recommendations are made with regard to the future use and continued development of the program.

- Users should be aware of the two basic numerical problems identified so far, i.e. the repeated roots problem and the convergence problem when modal truncation is used. When modal truncation is not used, convergence is not a problem.

- A detailed examination of the eigenvalue/eigenvector subroutines should be made to determine to what extent certain numerical problems can be eliminated by adding more sophisticated logic to the computational procedures. Appropriate modification to the code should be made.

- A means for testing the validity of computed eigenvalues and eigenvectors should be developed. An orthogonality check using the derived eigenvectors and input coefficient matrices is one possible means.

- The procedure developed in Section 3.7 for eliminating the low frequency convergence problem should be implemented in the DYNALIST II code.

- The other two convergence problems should be studied in depth with the objectives of providing reliable guidelines for selection of component modes, evaluation of resulting solution accuracy, and, if

possible, development of automatic convergence subroutines which complement the existing program.

The improvements and extended capabilities incorporated in DYNALIST II are believed to represent a major advance in the state-of-the-art of rail vehicle dynamic analysis. It is expected that specific user feedback will be very helpful in charting the continuing development of this program.

- APPENDIX A -

EQUATIONS OF MOTION FOR A RIGID WHEELSET

A.1 Description of System

Figure A-1 shows a single wheel-axle system. Imagine two sets of unit vectors; $\hat{e}_1$ and $\hat{e}_2$, are fixed to the rail and $\hat{i}_1$ and $\hat{i}_2$ are fixed to the axle. Two coordinates, p_1 and p_2, define the position of the axle with respect to the rail at any instant of time. These coordinates are:

p_1 = lateral displacement of axle from the center line of the rail system.

p_2 = rotation (radians) of the axle with respect to the rails.

The following parameters are also used in this appendix:

r_o = nominal radius of each wheel

V = Mean forward velocity of axle

λ_o = cone angle (radians) of each wheel

A.2 Velocities of Wheels

When the axle is rolling straight down the rails and $p_1 = p_2 = 0$ then each wheel rotates with the same angular velocity, ω_o, and the radius of the wheel which is in contact with the rail is the nominal radius of the wheel, r_o. As the axle displaces from this central position the contact radius either increases or decreases. The change in radius is a function of the lateral displacement and the wheel's cone angle, i.e. $\lambda_o p_1$. Since the angular velocity of the rigid wheelset is a constant, ω_o, it then follows that the rolling velocities of the wheels are:

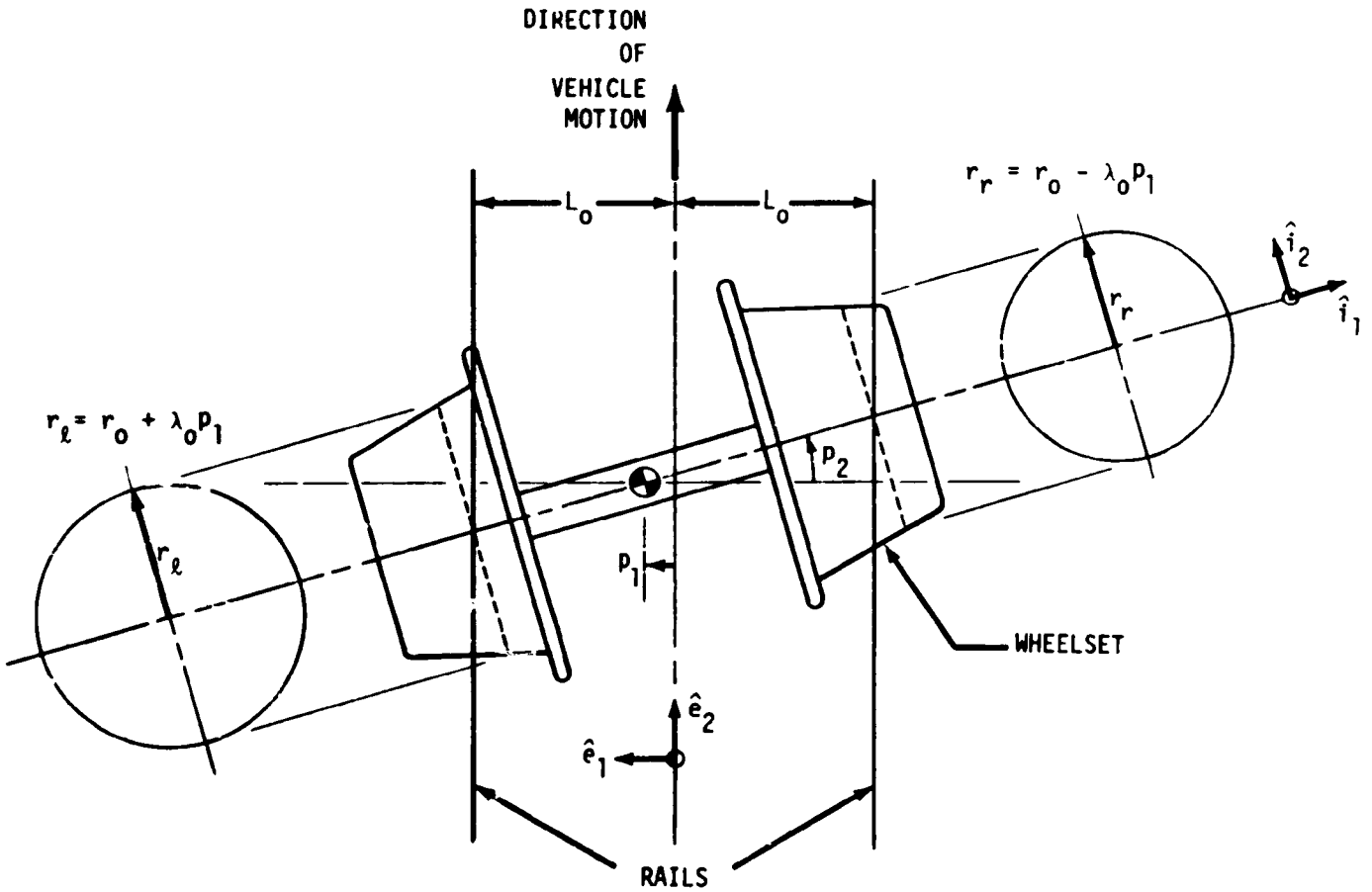

Figure A-1. Schematic of Wheel-Rail Contact Geometry

$\hat{V}_{R\ell}$ = rolling velocity of the left wheel

= ω_o (left contact radius)

= $\omega_o (r_o + \lambda_o p_1) \hat{i}_2$ (A-1)

$\hat{V}_{Rr}$ = rolling velocity of the right wheel

= ω_o (right contact radius)

= $\omega_o (r_o - \lambda_o p_1) \hat{i}_2$ (A-2)

The unit vector systems are such that for small displacements p_1 and p_2 it follows that:

$$\hat{i}_2 = p_2 \hat{e}_1 + \hat{e}_2 \quad \text{(A-3)}$$

and therefore

$$\hat{V}_{R\ell} = \omega_o (r_o + \lambda_o p_1)(p_2 \hat{e}_1 + \hat{e}_2)$$
$$= (\omega_o r_o p_2)\hat{e}_1 + \omega_o (r_o + \lambda_o p_1)\hat{e}_2 + 0^+ \hat{e}_1 \quad \text{(A-4)}$$

and

$$\hat{V}_{Rr} = \omega_o (r_o - \lambda_o p_1)(p_2 \hat{e}_1 + \hat{e}_2)$$
$$= (\omega_o r_o p_2)\hat{e}_1 + \omega_o (r_o - \lambda_o p_1)\hat{e}_2 + 0^+ \hat{e}_1 \quad \text{(A-5)}$$

In the above equations, 0^+ denotes the neglected higher order terms in p_1 and p_2.

The previous discussion pertains to the rolling velocity of each wheel. When creep occurs, the actual velocities are slightly different than the rolling velocities. The actual wheel velocities are,

$\hat{V}_{A\ell}$ = actual velocity of the left wheel

$$= (\dot{p}_1)\hat{e}_1 + (V - L_o \dot{p}_2)\hat{e}_2 \quad \text{(A-6)}$$

and

V_{Ar} = actual velocity of the right wheel

$$= (\dot{p}_1)\hat{e}_1 + (V + L_o\dot{p}_2)\hat{e}_2 \qquad \text{(A-7)}$$

If the actual and rolling velocities of each wheel were identical, then there would be no creep forces applied to the wheels. When the two velocities are not the same, creep forces are developed.

A.3 Creep Forces on a Wheelset

The creep forces acting on a wheel are proportional to the difference between the actual and rolling velocities of the wheel. It is customary to write this relationship in the following way:

$$\hat{F} = \text{creep force} = -f\left(\frac{\text{Actual Velocity - Rolling Velocity}}{\text{Mean Forward Velocity}}\right) \qquad \text{(A-8)}$$

where f denotes the creep coefficient.

The creep forces acting on the wheelset follow from the substitution of (A-4) to (A-7) in (A-8), i.e.

$\hat{F}_\ell$ = creep force on left wheel

$$= -(f/V)\,[\dot{p}_1\hat{e}_1 + (V - L_o\dot{p}_2)\hat{e}_2 - \omega_o r_o p_2\hat{e}_1 - \omega_o(r_o + \lambda_o p_1)\hat{e}_2]$$

$$= -f/V\,[\dot{p}_1 - Vp_2]\hat{e}_1 + f/V[L_o\dot{p}_2 + V(\lambda_o/r_o)p_1]\hat{e}_2 \qquad \text{(A-9)}$$

$\hat{F}_r$ = creep force on right wheel

$$= -f/V\,[\dot{p}_1 - Vp_2]\hat{e}_1 - f/V[L_o\dot{p}_2 + V(\lambda_o/r_o)p_1]\hat{e}_2 \qquad \text{(A-10)}$$

where by definition

$$V = \omega_o r_o \qquad \text{(A-11)}$$

A.4 Equations of Motion - No Rail Irregularities

The forces due to creep which act on the axle are given in (A-9) and (A-10). With the mass and mass moment of inertia (about its center) of the axle denoted by M and I, it follows directly that the scalar dynamical equations of motion are:

$$M\ddot{p}_1 = -f/V[\dot{p}_1 - Vp_2] - f/V[\dot{p}_1 - Vp_2]$$

or

$$M\ddot{p}_1(t) + (2f/V)\dot{p}_1(t) - (2f)p_2(t) = 0 \qquad \text{(A-12)}$$

and

$$I\ddot{p}_2 = -fL_o/V[L_o\dot{p}_2 + V(\lambda_o/r_o)p_1]$$
$$-fL_o/V[L_o\dot{p}_2 + V(\lambda_o/r_o)p_1]$$

or

$$I\ddot{p}_2(t) + \left(\frac{2fL_o^2}{V}\right)\dot{p}_2(t) + \left(\frac{2fL_o\lambda_o}{r_o}\right)p_1(t) = 0 \qquad \text{(A-13)}$$

Examination of (A-12) and (A-13) shows that coupling exists between the two coordinates through the displacement terms. No coupling exists between the acceleration and velocity terms.

A.5 Equations of Motion - Rail Irregularities

Equations (A-12) and (A-13) reflect the homogeneous differential equations of motion for motion down a straight rail. Figure A-2 shows schematically the rail irregularity with the coordinates

δ = lateral displacement of rail irregularity

$\delta' = d\delta/dx$ = slope of rail irregularity

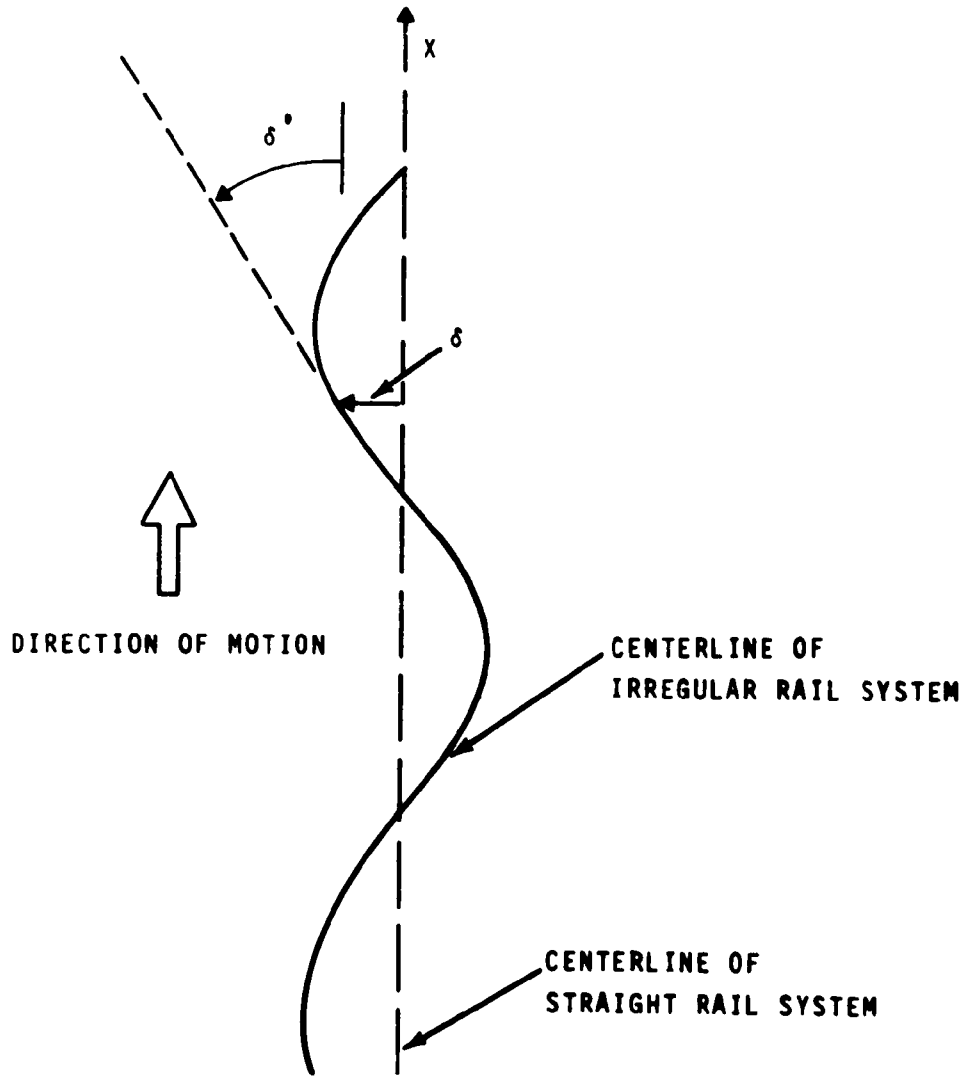

Figure A-2 Shape of Irregular Rail Centerline

In general, irregularities of the two rails are not the same. There may be some degree of correlation, particularly at larger wavelengths, but the irregularities are not identical. In any case, the irregularities may be represented as the sum of two functions, one symmetric with respect to the nominal centerline of the track, and the other antisymmetric. Since the symmetric rail irregularities induce no lateral motion, only the antisymmetric function need be considered for the lateral model. This argument justifies the representation of rail irregularities in terms of an irregular centerline, as shown in Figure A-2.

In order to derive equations of motion for a wheelset in the case of irregular rails, creep forces are considered to depend on the relative motion between wheels and rails. Equation (A-12) is therefore written

$$M\ddot{p}_1 + \frac{2f}{V}\left(\dot{p}_1 - \dot{\delta}\right) - 2f\left(p_2 - \delta'\right) = 0 \qquad \text{(A-14)}$$

From the relationship

$$\delta' = \frac{d\delta}{dx} = \frac{d\delta}{dt}\frac{dx}{dt} = \frac{\dot{\delta}}{V} \qquad \text{(A-15)}$$

Equation(A-14) is seen to reduce to

$$M\ddot{p}_1 + \frac{2f}{V}\dot{p}_1 - 2fp_2 = 0 \qquad \text{(A-16)}$$

which is identical to (A-12).

To write Equation (A-13) in terms of relative wheel-to-wheel motion, one must be careful in the direct application of formal substitution which leads to

$$I\ddot{p}_2 + \frac{2fL_o^2}{V}\left(\dot{p}_2 - \dot{\delta}'\right) + \frac{2fL_o\lambda_o}{r_o}\left(p_1 - \delta\right) = 0 \qquad \text{(A-17)}$$

Recognizing that

$$\dot{\delta}' = \frac{d}{dt}\left(\frac{d\delta}{dx}\right) = \frac{d}{dt}\left(\frac{d\delta}{dt}\frac{dt}{dx}\right) = \frac{1}{V}\ddot{\delta}$$

one would find

$$\ddot{I}p_2 + \left(\frac{2fL_o}{V}\right)\dot{p}_2 + \left(\frac{2fL_o\lambda_o}{r_o}\right)p_1 = \left(\frac{2fL_o^2}{V^2}\right)\ddot{\delta} + \left(\frac{2f\lambda_o L_o}{r_o}\right)\dot{\delta} \quad \text{(A-18)}$$

and conclude that <u>in the case of cylindrical wheels</u> where $\lambda_o = 0$, an irregular track excites wheelset motion. This is known to be untrue.

Some insight may be gained by contemplating the design of a test facility to simulate wheel-rail interaction. Suppose, first, that two circumferential rails are welded to a cylindrical drum which rotates about its axis fixed in a horizontal plane. If the drum spins at a constant rate, and a wheelset is placed on top of the rails, and constrained so that it cannot move forward or backward, but only in the lateral and yaw directions, the condition of a wheelset moving along straight track is simulated. The equations of motion for the wheelset would be given by (A-12) and (A-13).

If the drum were made to move with an oscillatory lateral motion $\delta(t)$ without yawing, then the equations of motion would be given by (A-14) and (A-17) with the δ' and $\dot{\delta}'$ terms both set equal to zero. Clearly, this motion of the drum does not simulate a wavy track because $\dot{\delta}$ appears in the equation containing $\ddot{p}_1$, whereas, in the case of a wavy track, (A-16) applies.

If the drum were a given a yaw degree of freedom in addition to lateral and spin, and the yaw angle $\delta'(t)$ were synchronized with $\delta(t)$ <u>in an attempt</u> to simulate wavy track, then the wheelset equations of motion would be given by (A-16) and (A-18). Since it has already been concluded that these equations do not represent a wheelset rolling on wavy track because the wheelset is forced when $\lambda_o = 0$, this type of drum motion must not simulate wavy track either.

In order to properly simulate the wavy track condition, one should be able to pass a planar surface over the rails on the moving drum in such a way that no slip (or creep) occurs at the contact points. This, of course, requires that one more degree of freedom be added to the drum, differential spin between the two rails. Then the motion is analogous to that of the rear wheels of an automobile zig-zaging down a straight road. The differential allows the rear wheels to turn at different rates as the car turns. Without the differential, the tires would tend to creep on the pavement, giving rise to creep forces and causing the tires to wear.

Returning to the problem of writing equations of motion for a wheelset on irregular track, one can now see that another term must be included in (A-17) to account for track curvature, $\delta'' = 1/\rho$ where ρ is defined to be the "instantaneous" radius of curvature at some point on the track. The creep force on the right wheel in the $\hat{e}_2$ direction is therefore

$$\hat{F}_r \cdot \hat{e}_2 = - \frac{fL_o}{V} \left[\dot{p}_2 - \left(\dot{\delta}' - \frac{V}{\rho} \right) \right]$$

However, since

$$\frac{V}{\rho} = V\delta'' = V \left(\frac{\dot{\delta}'}{V} \right) = \dot{\delta}'$$

it follows that

$$\hat{F}_r \cdot \hat{e}_2 = \frac{-fL_o}{V} \dot{p}_2$$

and similarly for the left wheel

$$\hat{F}_\ell \cdot \hat{e}_2 = \frac{fL_o}{V} \dot{p}_2$$

Finally then, for the case of a wheelset rolling on irregular rails with a centerline displacement given by $\delta(t)$, the equations of motion are

$$\ddot{M}p_1 + \left(\frac{2f}{V}\right)\dot{p}_1 - \left(2f\right)p_2 = 0 \qquad \text{(A-16)}$$

$$\ddot{I}p_2 + \left(\frac{2fL_o^2}{V}\right)\dot{p}_2 + \left(\frac{2fL_o\lambda_o}{r_o}\right)p_1 = \left(\frac{2fL_o\lambda_o}{r_o}\right)\delta \qquad \text{(A-19)}$$

Thus, when $\lambda_o = 0$, the wheelset is not excited. These equations agree with those presented in [11].

In retrospect, this circuitous derivation of creep forces in the case of irregular rails might be shortcut by developing a more suitable definition of creep.

- APPENDIX B -

CDC - 6600 TO DEC SYSTEM - 10 CONVERSION AND
CALCOMP PLOTTER COMPATIBILITY

The DYNALIST II computer program is currently operational on a Control Data Corp. 6600 computer system. Briefly, DYNALIST II requires a large amount of core (200K Octal) to compile and run. It uses available core space efficiently by using an Overlay structure. By saving the Overlay structure on a permanent file it is possible to run the program using less than 160 K Octal of core. The program requires three working tapes or disks in addition to those required by the standard input, output and plotting devices.

The Digital Equipment DEC System - 10 computer system currently installed at DOT-TSC has over 250 K Octal core memory available to the user. This is more than enough to compile and run DYNALIST II using any Overlay loading technique. DYNALIST II uses main, primary and secondary overlays. The configuration of these is shown in Figure B-1. Figure B-1 should demonstrate the feasibility of running this program on the DEC System - 10 The DEC System - 10 currently has three disk drives which is the minimum number needed to run the program efficiently. A list of possible considerations in the conversion from a CDC 6600 to a DEC System - 10 is given below.

B-1. It will not be possible to run DYNALIST II in double precision since DYNALIST II uses complex arithmetic. The DEC System -10 does not have double precision - complex variables nor does it allow mixed mode arithmetic between complex and double precision variables.

B-2. Operating in single precision, mixed mode arithmetic should cause no problems.

OVERLAY DESIGNATION

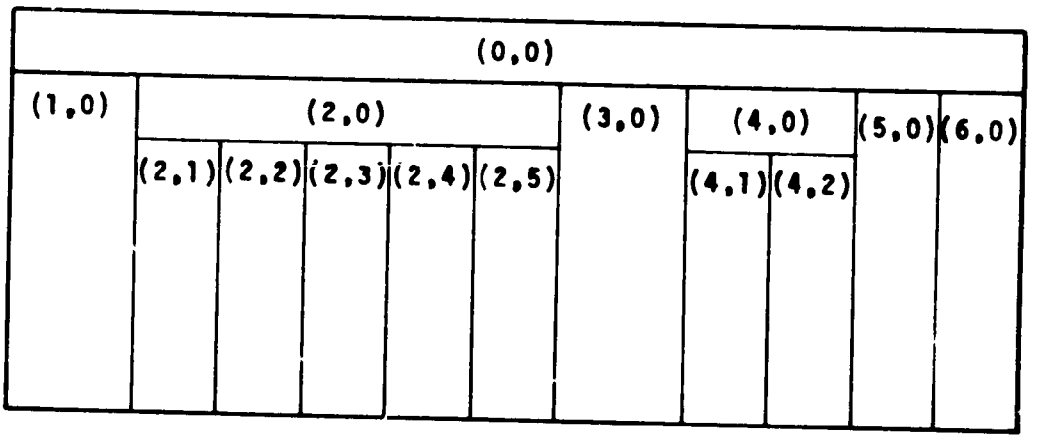

Figure B-1 DYNALIST II Overlay Structure

B-3. All library subroutines required are available on the DEC System - 10.

B-4. DYNALIST II uses six-character subroutine and variable names which is standard in FORTRAN IV. These would have to be shortened only if an incompatibility exists with regard to the DEC System - 10 Fortran compiler.

B-5. The DEC System - 10 accepts only 5-character Hollerith variables whereas the CDC - 6600 accepts 10-character Hollerith variables. This should affect only the title card.

B-6. Return statements in primary and secondary overlays and in subroutines may have to be replaced by transfers to the End statement.

B-7. DYNALIST II uses Tape 5 as input Tape 6 as output and Tape 10, Tape 11 and Tape 12 as working files. These may have to be renumbered.

B-8. Program cards may have to be changed or deleted.

B-9. DYNALIST II uses multiply-subscripted arrays in the same subroutines. This may cause problems.

B-10. If the DEC System - 10 on line CalComp Plotter routines are used, the following changes must be made in Overlay (4,2)

B-10.1. Eliminate CALL FACTOR (SIZE) and delete plot reduction option.

B-10.2. Account for lack of 999. continuation feature in the NUMBER routine.

B-10.3. SCALE routine must be changed and made compatible with AXIS routine.

B-10.4 A CALL PLOTS statement must be added to dimension a plotting buffer.

B-11. If the off-line Standard CalComp Plotter is used, only the CALL PLOTS statement need be added.

B-12. To use the CalComp log-log plotting routine the FREQ array will have to be converted back to an arithmetic scale, but not before being used in any CALL to SUBROUTINE MSR.

The arrays UPSD, TRACK and AMP need not be converted to a logarithmic scale but may be left in their arithmetic form. Note that the response program operates by using a constant frequency increment on a logarithmic scale and that this should not be altered.

- APPENDIX C -

SAMPLE PROBLEM

DYNALIST input data for the four degree-of-freedom lumped mass model described in Section 3.2 is derived in this appendix. All data begin in column 2. See User's Manual.

Title Card

Card 1: LUMPED MASS MODEL

Generate Component Data

Namelist block START contains four parameters as indicated in Section IV of the User's Manual. All parameters must be assigned values unless default options are desired or earlier entries have been made. The first step in solving a DYNALIST problem is to create a component data file. This is done in Segment 1 of the program which is called by specifying NTYPE = 1. Assuming that a new data file is to be created, the user will set NEWTAP = 0. No intermediate printout is desired so IFOUT = 0. If IRESP is not specified, it will default to 0. Thus, Card 2 becomes

Card 2: $START NTYPE = 1,NEWTAP = 0, IFOUT = 0,$

Having entered Segment 1, the parameters in Namelist Block COMPO must be specified. The first call to Segment 1 will generate the first component on the data file which is defined in accordance with Figure 3-1. This component may be designated by the "name" COMNAM = 1.00. The automatic matrix generator will not be used. Therefore IGEN = 0. Three coordinates, NU = 3, are required to define the motion of Component 1. One is the "constraint" coordinate which will attach to mass #3 and the other two define motion of masses #1 and #2 and are considered to be "free" coordinates. No rigid body coordinates are required. Namelist Block COMPO is initiated with the card

Card 3: $COMPO

Namelist parameters in this block may now be specified in any order. Thus we choose

Card 4: COMNAM=1.00,IGEN=0,NU=3,NCON=1,NRIGS=0,NFREE=2,

Coefficient matrices are entered in the p-coordinate system which in this case is chosen to represent physical coordinates so that the matrix PHI can be an identity matrix.

Card 5: PHI(1,1)=1,PHI(2,2)=1,PHI(3,3)=1,

All coefficient matrices are symmetric so the user may specify

Card 6: ISYMC=1,ISYMK=1,

The mass, damping and stiffness matrices for Component 1 are found from Figure 3-1 to be

$$m = \begin{bmatrix} 0 & 0 & 0 \\ 0 & 1 & 0 \\ 0 & 0 & 1 \end{bmatrix}$$

$$c = \begin{bmatrix} .01 & 0 & -.01 \\ 0 & .04 & -.02 \\ -.01 & -.02 & .03 \end{bmatrix}$$

$$k = \begin{bmatrix} 1 & 0 & -1 \\ 0 & 2 & -1 \\ -1 & -1 & 2 \end{bmatrix}$$

The constraint coordinate must come first followed by the free coordinates which are ordered as mass #1 followed by mass #2. Thus the next three cards are

Card 7: AMASS(2,2)=1, AMASS(3,3)=1,

Card 8: DAMP(1,1)=.01, DAMP(2,2)=.04, DAMP(1,3)=-.01,-.02,.03,

Card 9: STIFF(1,1)=1, STIFF(2,2)=2, STIFF(1,3)=-1,-1,2,

This completes Namelist Block COMPO for Component 1. The namelist block is terminated by the card

Card 10: $END

Component 2 data are placed on the data file in a similar fashion by entering Segment 1 again. This time NEWTAP = 1 since the data are to be placed on the same data file.

Card 11: $START NTYPE=1,NEWTAP=1,IFOUT=0,$

Data for Component 2 are entered again in Namelist Block COMPO. As before, the equations are entered in the physical coordinate system. Two coordinates are required, NU = 2. No component modes will be computed in this case so NFREE = 0. The user may choose to define the two coordinates as either rigid body or constraint coordinates; say he chooses the former. Then NCON = 0, NRIGS = 2. Thus

Card 12: COMNAM=2.00,IGEN=0,NU=2,NCON=0,NRIGS=2,NFREE=0,

Card 13: PHI(1,1)=1,PHI(2,2)=1,

If the coordinates are ordered so as to place mass #3 followed by mass #4, the coefficient matrices for Component 2 are

$$m = \begin{bmatrix} .5 & 0 \\ 0 & .3 \end{bmatrix}$$

$$c = \begin{bmatrix} .01 & -.01 \\ -.01 & .01 \end{bmatrix}$$

$$k = \begin{bmatrix} 1 & -1 \\ -1 & 1 \end{bmatrix}$$

The next four cards are therefore

Card 14: ISYMC=1,ISYMK=1,

Card 15: AMASS(1,1)=.5,AMASS(2,2)=.3,

Card 16: DAMP(1,1)=.01, DAMP(1,2)=-.01,.01,

Card 17: STIFF(1,1)=1, STIFF(1,2)=-1,1,

The COMPO data block is terminated by

Card 18: $END

Component Mode Truncation

Component modes may be truncated by entering Segment 2. This is accomplished by specifying NTYPE=2 in Namelist Block START

Card 19: $START NTYPE=2,IFOUT=0,$

Editing information is supplied in Namelist Block EDITT. The number of first order modes to be retained for each component is entered in the vector NMODE2 while the mode numbers for each component are entered in columns of the matrix MODES. Component 1 has 2 second order degrees of freedom and therefore has 4 first order modes. The user may wish to retain all of them. No modes were computed for Component 2 so none can be retained. The user will thus specify

Card 20: $EDITT

Card 21: NMODE2(1)=4,0,

Card 22: MODES(1,1)=1,2,3,4,

Card 23: $END

Synthesis

Upon completion of modal editing, the synthesis operation is performed to couple the components together and compute system modes. This is done in Segment 3 which is called by specifying NTYPE=3 in Namelist Block START. IFOUT has already been set equal to zero and does not have to be respecified. Since frequency response is to be computed, the user will set IRESP=1.

Card 24: $START NTYPE=3,IRESP=1,$

The number of components in the system is two so NCOMP=2. The identification of components and their order is specified by setting PRENAM(1)=1,2. There will be one constraint equation so NROWG = 1. If coordinate #1 of Component 1 is defined to be the dependent coordinate to be eleminated, then KDEP = 1. The u-coordinate vector for the system is

$$\{u\} = \begin{Bmatrix} u_1 \\ u_2 \\ u_3 \\ u_4 \\ u_5 \end{Bmatrix} = \begin{Bmatrix} u_1^1 \\ u_2^1 \\ u_3^1 \\ u_1^2 \\ u_2^2 \end{Bmatrix}$$

The two components are connected by specifying the compatibility constraint

$$u_1^1 = u_1^2 \quad \text{or} \quad u_1 - u_4 = 0$$

Therefore the user will specify G(1,1)=1,0,0,-1.

This information is entered in Namelist Block SYN.

Card 25: $SYN

Card 26: NCOMP=2,PRENAM=1,2,NROWG=1,KDEP(1)=1,

Card 27: G(1,1)=1,0,0,-1,

Card 28: $END

Response Computation

Response computations are made in Segment 4 by entering NTYPE=4 in Namelist Block START.

Card 29: $START NTYPE=4,$

Data are entered in Namelist Block SHAKE. The lower limit of the frequency range is .01 Hz and is specified by OMIN=.01. The upper limit of 1000 Hz is specified by OMAX=1000. Two hundred frequency response points are computed by specifying NSTEP=200. In order to compute acceleration frequency response, specify KIND=2. Force is input at only one coordinate so NAXLE =1, Since the end mass is associated with coordinate u_5 (note that coordinate numbering is different than in Figure 3-1 due to the extra constraint coordinate), LAXLE(1)=5. The magnitude of the force is unity and is entered as FORC0(1)=1. The vector FORC0 is used rather than FORC1 or FORC2 because it is not desired to multiply by $(i\Omega)$ or $(i\Omega)^2$. Since force is applied at only one point, phasing is of no concern; therefore PHASE may be ignored. It is desired to evaluate the frequency response of only the end mass, u_5, so that NLOOK=1 and LOOK=5. If neither sine response nor random response computations are desired and the user wishes to plot frequency response, then IPLOT=1 and NPLOT(1)=5. For notebook size plots (8 inch) set SIZE=8. The cards comprising Namelist Block SHAKE are

Card 30: $SHAKE

Card 31: OMIN=.01,OMAX=1000,NSTEP=200,

Card 32: KIND=2,NAXLE=1,LAXLE(1)=5,

Card 33: FORC0(1)=1,NLOOK=1,LOOK(1)=5,

Card 34: IPLOT=1,NPLOT(1)=5,SIZE=8,

Card 35: $END

Terminate Execution

Execution is terminated by specifying NTYPE=5 in Namelist Block START

Card 36: $START NTYPE=5,$

- APPENDIX D -

REPORT OF INVENTIONS

In accordance with the patent rights clause of the terms and conditions of this contract, and after a comprehensive review of the work performed, it was found that no new inventions, discoveries, or improvements of inventions were made.

REFERENCES

1. "High-Speed Ground Transportation Systems Engineering Study: Dynamic Analysis of Multiple Car Vehicles Using Component Modes," TRW Systems Group, July, 1970.

   Vol. I - "Analysis," Hasselman, T.K., Riead, H.D. and Kaplan, A., TRW Report No. 06818-6048-R0-00, DOT No. FRA-FT-71-43, Avail. NTIS PB 193545.

   Vol. II- "Parametric Study," Hasselman, T.K. and Kaplan, A., TRW Report No. 06818-6049-R0-00. DOT No. FRA-RT-71-53, Avail. NTIS PB 194375.

2. Hasselman, T.K. and Kaplan, A., "Train Dynamics by Complex Mode Synthesis," Joint ASME/ASCE Transportation Conference, Seattle, Washington, Paper No. 1487, July 1971.

3. Matsudaira, T., "How Can Train Speed Be Increased?", Japanese Railway Engineering, Vol. 7, No. 2, June 1966.

4. Houbolt, J.C., "Runway Roughness Studies in the Aeronautical Field," Air Transport Division, ASCE, March 1961.

5. Kaplan, A., Koval, L.R., and Choy, F., "Rail Vehicle Dynamics Analysis for High Speed Ground Transportation Roadbed Study," TRW Technical Report No. EM 17-22, September 1967.

6. Hurty, W.C., Collins, J.D., and Hart, G.C., "Dynamic Analysis of Large Structures by Modal Synthesis Techniques," J. Computers and Structures, Vol. 1, 1971.

7. Hasselman, T.K. and Kaplan, A., "Dynamic Analysis of Large Systems by Complex Mode Synthesis," ASME Journal of Dynamic Systems, Measurement and Control, September 1974.

8. Hasselman, T.K. and Hart, G.C., "A Minimization Method for Treating Convergence in Modal Synthesis", AIAA J., Vol. 12, No. 3, March 1974.

9. MacNeal, R.H., "A Hybrid Method of Component Mode Synthesis," Computers & Structures, 1, 1971, pp. 581-601.

10. Rubin, S., "An Improved Component-Mode Representation," AIAA/ASME/SAE 15th Structures, Structural Dynamics and Materials Conference, Las Vegas, Nevada, April 17-19, 1974.

11. Weinstock, H., "Analysis of Rail Vehicle Dynamics in Support of the Wheel Rail Dynamics Research Facility," DOT/UMTA Interium Report No. MA-06-0025-73, June 1973.